

# Late Holocene Sedimentation Dynamics in the Lake Ulaan Basin, Southern Mongolia: A History of a Playa Lake

Alexander Orkhonselenge (✉ [rkhnsing@num.edu.mn](mailto:rkhnsing@num.edu.mn))

National University of Mongolia <https://orcid.org/0000-0003-2501-8808>

Munkhjargal Uuganzaya

National University of Mongolia

Tuyagerel Davaagatan

Mongolian Academy of Sciences



---

## Research Article

**Keywords:** Lake Ulaan, Ongi River, Playa, Aeolian, Govi, Mongolia

**Posted Date:** February 25th, 2021

**DOI:** <https://doi.org/10.21203/rs.3.rs-256808/v1>

**License:**   This work is licensed under a Creative Commons Attribution 4.0 International License. [Read Full License](#)

---

# Abstract

Sedimentation dynamics in the Lake Ulaan basin located in the northern margin of the Govi region, southern Mongolia show high sedimentation rates of 11.8–22.7 cm/ka in the eastern part of the basin and low rates of 3.3–5.8 cm/ka in the western part during the late Holocene. The eastern and western parts of the lake have been strongly influenced by fluvial and aeolian activities since the arid late Holocene. However, fluvial sediment input was more significantly recorded in the eastern part. Aeolian deflation has been prevailing throughout the lake bank recently. Lake Ulaan reached its maximum extent before the early Holocene (Sternberg and Paillou, 2015; Holguin and Sternberg, 2016) with a water depth of ~43 m (Lehmkuhl et al., 2018a). After the early Holocene, Lake Ulaan started to decrease its area, and the drop of the lake level intensified since the middle Holocene. In the late Holocene, the western and eastern parts were initially exposed to wind deflation at 2.7–3.2 cal. ka BP and the aerial exposition continued at 0.6–1.3 cal. ka BP. In the Anthropocene, Lake Ulaan has rapidly shifted into a playa lake condition during the last five to six decades, and it has become an open-source area of dust generation blown out by the westerly winds.

## 1. Introduction

Lake sediments can reconstruct regional environmental and climate changes during the geological period because the lake is a container, an accumulator, and a repository. Autochthonous and allochthonous lake sediments can provide records of both lake and its basin responses to climate change (Dearing 1994). The mineral component of lake sediments would reflect the intensity of erosion in the basin (Roberts 1998). Moreover, exposed paleolake deposits allow us to find out the origin and provenance of the lake sediments (Einsele 1992).

Boundaries of natural regions in semiarid Mongolia, particularly the Govi (or Gobi)[1] region, are shifting from the south to the north by year due to an abrupt rise in average air temperature by 1.7–2.5°C/yr (Dulamsuren 2016). The Govi region's landscape in southern Mongolia is rapidly changing from the Govi to the desertic condition. The development of the Khongor sand dunefield in southern Mongolia at 4.0 ka BP (Felauer et al. 2012) implies that the playa environment in the Govi region started to form at that time. According to Baker (2007), a playa environment is a flat-bottom depression, consisting of a **dry lake**, in interior desert basins in arid and semiarid regions. Globally, the playa environment is periodically covered by water that slowly filtrates into the groundwater or evaporates into the [atmosphere](#) (Baker 2007; Komatsu et al. 2007).

Southern Mongolia is climatologically important because variations in the Mongolian High-Pressure System's intensity have strongly controlled Central Asian regional climate during the Quaternary Period (Owen et al. 1997). The Govi region's climate has been generally arid in the Quaternary (Berkey and Morris 1927). The average air temperature is –15°C to –25°C in January and 20–25°C in July, and the average precipitation is less than 100 mm/yr (Tserensodnom 1971). The average rainfall is 50–150 mm/yr, and the open water evaporation is 1000–1300 mm/yr in the Govi desert region (Ministry of Environment and Green Development 2013). The observed warming trend shows that the average air temperature has risen by 1.6–1.7°C/yr in the Govi desert from 1940 to 2001 (Batima et al. 2005). Severe droughts in the eastern Govi region, observed since the late 1990s, have intensified the groundwater level and lake area (Kang et al. 2015). Climate data observed at meteorological stations in the Valley of Lakes during 1975–2015 show trends in temperature rise

since 1995 and precipitation fluctuations since 1975 (Orkhonselenge et al. 2018a). Rivers, feeding lakes in the Govi region, decrease in discharges in all seasons at the present time (Davaa 2015). In the Govi region, river water temperature is expected to rise 2.5–2.7°C in 2020, 3.2–3.5°C in 2050, and 3.9–4.2°C in 2080 (Davaa 2010).

In recent years, Lake Ulaan has attracted numerous detailed studies in geomorphology, sedimentology, hydrology, and paleogeography. For instance, Lake Ulaan's water level dropped by 1–2 m since 1980 (Batnasan 1998), and the lake faced the challenge of the continuous decrease in its area due to the rising temperature over the last half-century (Orkhonselenge et al. 2018a). However, there has been little research about how sedimentation records past climates in the Lake Ulaan basin and its evolutionary history during the geological period. Up to now, little is known about the distribution and timing of the late Quaternary aeolian sediments. This study presents the late Holocene sedimentation rates in Lake Ulaan, associated fluvial and aeolian processes, hydrological evolution in the past, and when the lake has shifted into the playa environment.

## 2. Site Description

### *2.1 Geological setting*

Lake Ulaan basin is underlain by reddish sandstones over rhyolite flows and andesites (Berkey and Morris 1927) and the middle to late Quaternary deposits on the Neogene molasses deposits (Academy of Sciences of Mongolia and Academy of Sciences of USSR 1990) within the Proterozoic-Carboniferous lake zone (Guy et al. 2014). Lake Ulaan is tectonostratigraphically included in the Mandal Ovoo island arc terrane consisting mainly of the middle to late Paleozoic oceanic ophiolites, tholeiitic calc-alkaline volcanic, and volcano-clastic rocks overlain by non-marine sedimentary rocks (Badarch et al. 2002). Hills to the west and south of Lake Ulaan are composed mainly of Silurian limestone and dolomite and Cretaceous basalt and clastic sedimentary rocks, while to the east and north, the bedrock is dominated by Archaean and Paleoproterozoic metamorphic complexes and Paleozoic and Mesozoic sedimentary rocks (Academy of Sciences of Mongolia and Academy of Sciences of USSR 1990).

For geological formation, Lake Ulaan covers a continental platform consisting of Cenozoic red and gray terrigenous sands, gravels, and pebbles. It borders with Cenozoic limestone and basalts and Devonian terrigenous tuff greywacke in the southeast (Academy of Sciences of Mongolia and Academy of Sciences of USSR 1990). In the lake basin, Makhbadar (2012) identified early Cretaceous Manlai, Khukh Shiir, Ulziit, and Kholboot Formations, consisting of light grey and grey sandstone, ooze, siltstone, argillite, conglomerate, gravels, pyroxene basalt, and andesite. Surface sediments in Lake Ulaan are derived from a mafic igneous rock in an oceanic island arc setting (Lee et al. 2013).

### *2.2 Geomorphological setting*

Lake Ulaan is located at 1024 m a.s.l. in the eastern end of the Valley of Lakes between the Khangai and Govi Altai Mountain Ranges at the northern border of the Govi region in southern Mongolia (Fig. 1a). The modern topography of the Lake Ulaan basin formed in late Mesozoic graben-synclinal structure rift (Tserensodnom

2000) surrounded by Paleozoic linear uplifts (Narantsetseg et al. 2011). The Lake Ulaan basin is marshy in general, and it is located between relatively low hills at 1050–1110 m a.s.l. (Fig. 1b). Because this lake basin is at the lowest elevation in the Valley of Lakes (Orkhonselenge et al. 2018a), thick alluvial and lacustrine deposits were accumulated in the past (Tsegmid 1969).

Lake Ulaan is hypothesized as a deposition center for the whole lake basin system in the Valley of Lakes during the Quaternary (Tserensodnom 2000). Bottom sediments of Lake Ulaan consisted of deposits in the Neogene when water level and area were almost 100 m higher and several ten times larger in size than the present (Tserensodnom, 1971). Lake beaches are flat plain and swampy (Orkhonselenge et al. 2018b), and there are sand dunefields in the northwest and north (Tsegmid 1969). Dashzeveg et al. (2005) noted the Cretaceous dunefield in the Lake Ulaan basin based on cross-bedded intervals, occasionally exhibiting wind-ripple cross lamination in the Bayan Zag and Tugrugiin Shiree stratigraphic columns.

### *2.3 Hydrological setting*

Lake Ulaan is a terminal lake of Ongi River (Fig. 1b), draining from the Khangai Mountain Range (Fig. 1a). However, the river cannot permanently feed the lake today (Fig. 2g, h) due to the fluctuating precipitation; hence the lake area is often changed. The modern Lake Ulaan is apparently divided into the eastern and western parts separated by an approximately 6 km long and 0.5–2.0 km wide arcuate N-S trending spit (Fig. 3). The spit intersects the center of Lake Ulaan, dams the eastern part, and keeps its level ~0.5 m higher than that of the western part during heavy rainfall. The water from the Ongi River enters the eastern part directly, but it feeds the western part via crossing over the spit/three small channels (or spillways) in the spit (C1 to C3 in Fig. 3) or through groundwater.

Lake Ulaan holds a water resource of 0.158 km<sup>3</sup> (Tserensodnom 2000), but it is almost dried out during low precipitation (Fig. 2a, c). The lake has been a shallow playa lake, dry most of the year, and the lake floor was aerially exposed and vegetated (Fig. 2c, d). The lake reshrank in 1986–1989 (Batnasan 1998), 2010 (Davaa 2015), and 2015 (Fig. 2a). Lake Ulaan is generally a freshwater lake system even though it has no outflow, unlike other lakes in the Govi region (Tsegmid 1969). The lake water's freshness is related to the lake water flows through the unconsolidated soil around the lake under the highly evaporative climate condition (Tsegmid 1969). Nevertheless, according to Tsend (1965), lake water is mild, and the lake water is dominated by HCO<sub>3</sub><sup>-</sup> and Ca<sup>2+</sup>.

## **3. Material And Methods**

### **3.1 Field sampling**

During the fieldwork on 18 June 2018, we collected bulk samples from four sites on the exposed floor in the eastern part of Lake Ulaan (Fig. 3b). The first site (LU18-1) is located at 1029 m a.s.l., where the upper 35 cm samples were obtained. At the next site (LU18-2) at an elevation of 1029 m a.s.l., the upper 38 cm samples were collected. For the site (LU18-3) at 1030 m a.s.l., the upper 46 cm samples were obtained. At the last site (LU18-4) at 1028 m a.s.l., the upper 36 cm samples were collected. Stratigraphic columns with lithological description and color of the samples are shown in Fig. 4a.

As shown in Fig. 3b, the first two sites LU18-1 and LU18-2, are located in the lake's center, whereas the last two sites LU18-3 and LU18-4, are located toward the margins as in the case of the sites UN15-1 and UN15-2 (Fig. 3) for the previously studied by Orkhonselenge et al. (2018b). However, at present, the sites LU18-1 to LU18-4 in the eastern part of the lake (Fig. 3b) are situated under the condition which is more permanently inundated during rainfalls than those in the lake's western part, which has almost shifted to the drier playa condition (Fig. 3). It is confirmed that our four sampling sites are included in the current lake extent but were exposed at the time of our sampling (Fig. 2c) (see Figs. 3, 5, 7 in Holguin and Sternberg 2016).

The sites UN15-1 and UN15-2 at the exposed floor in the western part of the lake (Fig. 3) are situated at 4–6 m lower than those sites LU18-1 to LU18-4 in the eastern part of the lake (Fig. 5a). It implies the western part consists of the unconsolidated sediments, which are easily blown by winds, i.e., the erosion rate there may have been higher than that in the eastern part of the lake since 3.2 cal. ka BP (Orkhonselenge et al. 2018b) when it faced the first aerial exposure. Whereas, the deposition rate is higher in the eastern part of the lake (Fig. 4b) than that in the western part of the lake (Fig. 5b, c) because the eastern part of the lake is continuously overloaded/ fed by groundwater and discharge of Ongi River during the rainfall in addition to aeolian deposits today. The difference in a deposition is likely augmented by the presence of a spit that provides a physical barrier blocking the smooth transfer of runoff from the eastern part to the lake's western part (Fig. 3). The exposed floor in the western part of the lake (Fig. 2a) was covered by water in the Landsat 8 image in 2014 (Fig. 3a); however, the water coverage shifted to the east or left the western part of the lake in 2019 (Fig. 3b).

### 3.2 Major elements' analysis

Major elements of the lake sediments were analyzed at the Division of Radionuclide Analysis, the Central Geological Laboratory in Mongolia, using the Axios Max X-ray fluorescence (XRF) spectrophotometer. The major elements' functions and ratios of the lake sediments are used to create discriminant diagrams for studying the provenance of mafic and less-intermediate igneous (P1), intermediate igneous (P2), felsic igneous (P3), and quartzose sediments (P4) (e.g., Roser and Korsch 1988) in Fig. 6a; and tectonic setting of passive margin (PM), active continental margin (ACM), and oceanic island arc (ARC) (e.g., Roser and Korsch 1986) in Fig. 6b.

The geochemical classification diagram to clarify source rock composition is described based on  $\log[\text{SiO}_2/\text{Al}_2\text{O}_3]$  vs.  $\log[\text{Fe}_2\text{O}_3/\text{K}_2\text{O}]$  by Herron (1988) in Fig. 7a. The source rock composition can be estimated using the  $\text{Al}_2\text{O}_3\text{-CaO+Na}_2\text{O-K}_2\text{O}$  (A-CN-K) ternary diagram (Nesbitt and Young 1984) in Fig. 7b. The degree of weathering in the source area can be identified by the Chemical Index of Alteration (CIA:  $[\text{Al}_2\text{O}_3/(\text{Al}_2\text{O}_3+\text{Na}_2\text{O}+\text{K}_2\text{O}+\text{CaO})]\times 100$ ) in Fig. 7b. A high value indicates intensive weathering dominance (Harnois 1988) and a highly chemically weathered source area (Nesbitt and Young 1982). Moreover, a correlation between  $\text{SiO}_2$  and  $\text{Al}_2\text{O}_3+\text{K}_2\text{O}+\text{Na}_2\text{O}$  indicates the lake sediments' chemical maturity (Suttner and Dutta 1986).

### 3.3. Measurement of radiocarbon

Analysis for radiocarbon ( $^{14}\text{C}$ ) dating was conducted with the Accelerated Mass Spectrophotometry (AMS) at the Institute of Accelerator Analysis Ltd. in Japan. According to the laboratory report, the graphite sample was measured against a standard of Oxalic acid ( $\text{HOxII}$ ) provided by the National Institute of Standards and Technology, USA, using a  $^{14}\text{C}$ -AMS system based on the tandem accelerator. The samples with the plant fragments show sufficient carbon recovery values at 41.29–50.83% (Table 1).

For the calculation of  $^{14}\text{C}$  age, the Libby half-life of 5568 years was used (Stuiver and Polach 1977). Percent of modern carbon (pMC) refers to a ratio of the  $^{14}\text{C}$  concentration in the sample relative to 1950. Calibrated calendar age is a range of age corresponding to  $^{14}\text{C}$  age via a calibration curve produced from the  $^{14}\text{C}$  concentration of samples of known age. It is expressed by the  $1\sigma$  error range (68.2% probability) or the  $2\sigma$  error range (95.4% probability) in Table 2. The calibration in this study was conducted by OxCal v.4.3 (Bronk Ramsey 2009) based on IntCal13 database (Reimer et al. 2013).

## 4. Results

### 4.1 Provenance, tectonic setting, minerals, and weathering

The discriminant functions 1 and 2 to infer provenance in the Lake Ulaan basin were plotted (Fig. 6a) proposed by Roser and Korsch (1988). The Lake Ulaan sediments show a mafic igneous provenance at the site LU18-4, except for the surface sediments, and a quartzose sedimentary provenance at the sites LU18-1, 3, and UN15-1, 2, while both mafic igneous and quartzose sedimentary provenances at the site LU18-2. The result coincides with the mafic igneous rocks in an ARC setting for upper and lower sediments of Lake Ulaan and the quartzose sedimentary rocks derived from an ACM source for medium sediments (Lee et al., 2013).

The  $\text{SiO}_2$  content and  $\log[\text{K}_2\text{O}/\text{Na}_2\text{O}]$  of the Lake Ulaan sediments were plotted to decipher their tectonic settings (Fig. 6b) proposed by Roser and Korsch (1986). The result shows the ARC tectonic deposition environment for the Lake Ulaan sediments (Fig. 6b). According to McLennan et al. (1993), PM tectonic environment is characterized by felsic composition, while the ARC tectonic environments are typically enriched in mafic components. The Lake Ulaan sediments show the mafic igneous rocks formed in the ARC setting, except for the UN15-1 sediment (Fig. 6b).

The geochemical classification diagram shows that the Lake Ulaan sediments are mostly composed of shale, while the sediments at the sites UN15-1 and LU18-4 in the lake's margin consist of greywacke and litharenite (Fig. 7a). The A-CN-K ternary plot shows that the Lake Ulaan sediments were derived from the granitic to granodiorite source terrain in the eastern part of the lake and from the smectite source terrain in the western part of the lake (Fig. 7b). The granodiorite source is related to the composition of volcanic clastic sedimentary rocks. The lake sediments along the side towards the plagioclase (Fig. 7b) imply the Na-rich and Ca-rich feldspars' presence.

In the Lake Ulaan sediments, the CIA range from 55.88–63.28 at the sites LU18-1 to LU18-4 in the eastern part of the lake (Fig. 7b) to 60.24–62.64 at the sites UN15-1 and UN15-2 in the western part of the lake (Orkhonselenge et al. 2018b). The CIA values in the Lake Ulaan sediments indicate the low degree of source

area weathering in the lake's eastern part and the moderate to the high degree of source area weathering in the lake's western part (Fig. 7b).

The results from the source area provenance (Fig. 6a) and tectonic setting (Fig. 6b), and source rock compositions (Fig. 7a), and minerals and weathering intensity (Fig. 7b) are in agreement with the structure of the geological formation in the Lake Ulaan basin with the non-marine sedimentary rocks underlain by the oceanic ophiolites, tholeiitic to calc-alkaline volcanic and volcano-clastic rocks, bounded by limestone and basalts, and terrigenous tuff greywacke around the lake basin (see details in Section 2.2).

## 4.2 Age correction

In terms of age correction, selecting the material for dating depending on shallow or deep lakes is crucial for inferring erosion, transportation, and deposition in the lake basin. In deep lakes, terrestrial organic materials are redeposited by streams (Orkhonselenge et al. 2013). For example, in Lake Khuvsgul of northern Mongolia average ages of surface sediments are ca. 0.5 ka (Prokopenko et al. 2005), and  $^{14}\text{C}$  ages of bulk organics are 0.4–4.0 ka older than wood fragments (Watanabe et al. 2009). It is known that the dates obtained from plant fragments are more reliable than those obtained from bulk organics for age corrections (e.g., McGeehin et al. 2001). However, Orkhonselenge et al. (2018b) noted that plant macrofossils and wood fragments are applicable for precise dating if they are only found in deep sediments, and that the plants recently deposited in surface sediments are dated as modern. Moreover, the influx of  $^{14}\text{C}$ -deficient carbon delivered from adjacent soils and the Paleozoic carbonate rocks during the early to the late Holocene is still active in Lake Ulaan today (Lee et al. 2011).

In shallow Lake Ulaan, bulk sediments and plant fragments were chosen for establishing age datasets (Table 1). The plant fragments in the sediments (LU18-2: 18–20 cm, LU18-3: 25–28 cm, and LU18-4: 34–36 cm) are dated as modern (Table 1). The modern ages show the active aeolian and fluvial erosions and rapid sedimentations at the sites LU18-3, 4 in the lake's margin than the site LU18-2 in the center of the lake (Table 2). Therefore, the same lake sediments for obtaining precise dating and reconstructing depositional environments in the past, the bulk sediments are used for age corrections as the well-preserved sediments in the shallow Lake Ulaan (Orkhonselenge et al. 2018b). As described in Section 3.3, the samples with the plant fragments from all Lake Ulaan sites show sufficient carbon recovery (Table 1), i.e., the bulk sediments from Lake Ulaan can date the correct age and infer the sedimentation rates in the lake basin.

In the western part of Lake Ulaan the reservoir effect is negligibly corrected to be at 0.2 ka because of the terrestrials' input after removing the surface sediments by aeolian processes during the intensive drought in the late Holocene (Orkhonselenge et al. 2018b). However, in the eastern part of the lake, it is estimated at 0.1 ka, i.e., overall, the reservoir effect can be at 0.15 ka throughout Lake Ulaan. In addition to the previous calibrated age data by Orkhonselenge et al. (2018b), the calibrated data (Table 2) and the age to depth model (Fig. 8) are used for inferring sedimentation dynamics in the Lake Ulaan basin.

## 4.3 Radiocarbon dating

Tables 1 and 2 show the sediments' conventional and calibrated ages in the eastern part of Lake Ulaan. The conventional  $^{14}\text{C}$  ages with  $\delta^{13}\text{C}$  correction show modern to  $3020 \pm 30$  yr BP for bulk sediments with the pMC

between  $68.66 \pm 0.22\%$  and  $92.96 \pm 0.26\%$ , and the modern time for plant fragments with the pMC greater than  $102.77 \pm 0.27\%$  (Table 1). The calibrated ages of the  $^{14}\text{C}$  dating show 616 cal. BP, with a probability of 68.0% at the site LU18-1, 1010 cal. BP, with a probability of 95.4% and 3205 cal. BP, with a probability of 77.4% at the site LU18-2, 2381 cal. BP with a probability of 95.4% at the site LU18-3, and 1265 cal. BP, with a probability of 76.7% at the site LU18-4 (Table 2).

The calibrated ages allow us to infer that the near-surface sediments (5 cm depths) in the eastern part of Lake Ulaan deposited at 1010 cal. BP at the site LU18-2 in the central part and 1265 cal. BP at the site LU18-4 in the lake's marginal part (Table 2, Fig. 8a, c). In other words, the near-surface sediments at the same 5 cm depths were deposited at 1.0–1.3 cal. ka BP in the eastern part of the lake and at 2.7–3.2 cal. ka BP at the sites UN15-1, 2 in the lake's western part (Orkhonselenge et al. 2018b; Fig. 8b, d). However, the original near-surface sediments at 5 cm depths in the western part of the lake may have already been eroded and transported from there because the western part of the lake lies at ~4–6 m lower elevation (Fig. 5a). The calibrated ages of the  $^{14}\text{C}$  dating at the sediments deeper than 20 cm in the eastern part of the lake show 3205 cal. BP at the site LU18-2 in the center and 2381 cal. BP at the site LU18-3 in the margin of the lake (Fig. 8b, c). However, the ages at 20 cm depth sediments in the lake's western part show 6.0 cal. ka BP at the site UN15-1 and 3.4 cal. ka BP at the site UN15-2 (Orkhonselenge et al. 2018b; Fig. 8b, d). It implies that the deep sediments were deposited at 2.4–3.2 cal. ka BP in the eastern and 3.4–6.0 cal. ka BP in the western parts of the lake (Fig. 8).

Overall, the eastern part of Lake Ulaan shows ages 1.7–1.9 ka younger for the near-surface sediments than those in the western part, while the western part shows 2.8–3.6 ka older for the deep deposits (Fig. 8b). The  $^{14}\text{C}$  ages in the eastern part of the lake indicate that the near-surface sediment at the site LU18-2 in the center is 0.3 ka younger than the sediment at the site LU18-4 in the lake's margin. In comparison, the deeper sediment at the site LU18-2 at the center is 0.8 ka older than the deeper sediment at the site LU18-3 in the margin of Lake Ulaan (Fig. 8c). It implies that the younger at the site LU18-3 and older sediments at the site LU18-4 in the margin than those at the site LU18-2 in the center of the lake show rapidly deposited pulse sediments and well-preserved old sediments.

#### **4.4 Sedimentation rate**

In the center of Lake Ulaan, sedimentations at 14 cm depth of the site LU18-1 occurred at 0.6 cal. ka BP, whereas the sedimentations at 7 cm depth of the site LU18-2 occurred at 1.0 cal. ka BP and 38 cm depth at 3.2 cal. ka BP (Table 3, Figs. 4b, 5b, c). In the lake's margin, the sedimentations at 46 cm depth of the site LU18-3 occurred at 2.4 cal. ka BP and at 6 cm depth of the site LU18-4 occurred at 1.3 cal. ka BP (Table 3, Fig. 5b, c). In Lake Ulaan, as in other lakes in the Govi region, the sedimentation rates (Figs. 4b, 5b, c) should be a function of both sediment deposition and deflation by wind depending on the condition of water coverage and the annual precipitation input to the Ongi River (Fig. 2e, f) for its discharge and the groundwater. The center of the lake basin was more optimized for sediment preservation since it was more protected by water. Near the center of the basin, the sedimentation has been fast during the last 600 years at the site LU18-1, where the sedimentation rate shows a massive pulse of sedimentation with an average sedimentation rate of 22.75 cm/ka (Table 3, Figs. 4b, 5b, c). In another near center of the lake, the sedimentation rate is shown at 11.85 cm/ka at the site LU18-2 (Table 3, Figs. 4b, 5b, c). In the lake's margin, the sedimentation has been fast



at the rate of 19.32 cm/ka at the site LU18-3, but it has been remarkably recorded for a longer period (over 2400 years) (Table 3, Figs. 4b, 5b, c). In the meanwhile another margin site LU18-4 of the lake, the sedimentation rate was slow (4–5 cm/yr), but for a shorter period (for 1200–1300 years), i.e., the average sedimentation rate is 4.74 cm/ka at the site LU18-4 (Table 3, Figs. 4b, 5b, c).

The average sedimentation rates in the eastern part of the lake, except for the site LU18-4 (Fig. 4b), are indicated to have been at high levels and are comparatively larger than those of 3.3–5.8 cm/ka at the sites UN15-1 and UN15-2 (Orkhonselenge et al. 2018b) in the western part of the lake (Fig. 5b, c). In both western and eastern parts of Lake Ulaan, the sedimentation rates increase from the margin toward the lake's center (e.g., from UN15-1 to UN15-2, and from LU18-4 to LU18-1) (Fig. 5b, c). The lake margins have probably been more exposed to aeolian deflations than the lake center hence recording slower sedimentations. Still, other margin sites (e.g., LU18-3) may occasionally have higher sedimentations due to massive discharge pulses during the Ongi River's flooding (Fig. 2e, f) because Lake Ulaan is a terminal lake of the Ongi River. These giant pulses of sedimentations in the eastern part of the lake imply that this part of the lake has received precipitation-derived river water in addition to the glacier and permafrost meltwaters, whereas the western part of the lake may have been fed only by glacier meltwater via groundwater (Figs. 9, 10).

The sharp division of the eastern and western parts (Fig. 3) seems to be enhanced by the spit's presence separating the two areas by obstructing the free flow of surface water from the Ongi River. As strongly represented by the western part of the Lake Ulaan (Orkhonselenge et al. 2018b), the area in the late Holocene (Table 4, see Section 5.2) is characterized by increased aridity and decreased humidity (Orkhonselenge et al. 2018a), and consequently, the lake decreased in size (Holguin and Sternberg 2016) after 4.0 cal. ka BP (Felauer et al. 2012) as indicated by reduced fluvial processes and increased aeolian processes (Lee et al. 2011; 2013). This pattern is consistent with other lacustrine evidence from lakes in the Govi region (Felauer et al. 2012; Grunert et al. 2000).

## 5. Discussions

### 5.1 Sedimentation dynamics

The sedimentation rate in the eastern part of Lake Ulaan just near the downstream of Ongi River is remarkably higher than that of the western part (Fig. 8b) because the presently dried out Ongi River (Fig. 2g, h) may intermittently feed the lake with high meltwater discharge transporting sands (Fig. 9). The spits may block the sand transportation and water discharge, and it may slow down the fluvial sedimentation rate in the western part, where the filling by water is more significantly delayed than the eastern part (Figs. 3, 10). The eastern part tends to be covered with the water from the Ongi River and the groundwater for more extended periods and consequently have less aeolian deflation (Figs. 9, 10). The possibility of sand transport across the ice covering the lake in the Depression of Great Lakes in western Mongolia during the long winter (Stolz et al. 2012) when most of the sand storms caused by strong west and northwest winds (Hempelmann 2010) may support the aeolian sedimentations (i.e., deposition) in the Lake Ulaan area in winter and spring.

Lakes in the Depression of Great Lakes and the Valley of Lakes find high stands due to increased snowfall caused by a more humid climate resulting in a considerable glaciation at high elevations (Lehmkuhl and

Lang 2001; Lehmkuhl et al. 2018b). This snow accumulation may contribute to the meltwater runoff in spring and early summer and the fluvial sedimentations in the lake's eastern part (Fig. 9). However, the climate in the Lake Ulaan region still stays under the arid climate throughout the year (Figs. 11, 12) and permits deflation of the lake depression and strengthened aeolian sedimentation (Figs. 9, 10), probably increased by high wind velocities of up to 34–40 m/s (Amarjargal 2016) passing through the Valley of Lakes. The near-surface sediments of Lake Ulaan down to 3.9 m depth correspond to wind deposits (Lee et al. 2011) and are interpreted to be the lake terrain (Badarch et al. 2002). According to Lehmkuhl et al. (2018a), the silts deposited in Lake Ulaan during the humid middle Holocene may have been exposed to wind activity when the lake is dried out as a playa bed. The early to late Holocene sediments in the Lake Ulaan basin indicate the aeolian dominant sediment-transport mechanism (Lee et al. 2011). Moreover, the sediments in the Lake Ulaan basin were transported by local westerly winds blowing along the Valley of Lakes during the last 11.2 ka BP (Lee et al. 2013).

In general, the aeolian sedimentations predominated in the Lake Ulaan basin since the early Holocene. For instance, the fine aeolian sand at 4.2 m depth in a 6 m high terrace of Ongi River 55 km northeast of Lake Ulaan indicated that the deposition had already started during the late Glacial period (Lehmkuhl et al. 2018a). However, the fluvial sedimentation strengthened in the middle Holocene, and aeolian sedimentation increased during the late Holocene (Fig. 9). Some large alluvial fans or deltas may have formed around the Lake Ulaan basin in the past that are now buried by wind-derived surface sediments (Sternberg and Paillou 2015). The aeolian deflation in the Lake Ulaan basin during the Anthropocene (Figs. 9c, 10) had intensified since the 1950s because of the historical records of water coverage of Lake Ulaan (Table 4). Continuous deflations occurred in the Lake Ulaan basin in winter, spring, and autumn since that time, except for summer when the lake was filled due to rainfall in 1960, 1970, and 2013–2014 (Table 4, Fig. 2b, d). The lake has been an end-transfer base floor for aeolian sedimentations blown from the Depression of Great Lakes in the northwest through the Valley of Lakes, and also a continuous source for dust storms and suspension transport of silts towards the Pacific Ocean in the southeast.

## 5.2 Lake evolution history

Like other lakes in the Govi region, Lake Ulaan experienced significant changes in water level and coverage area during the late Quaternary. Historical analysis of changes in lake level and size (Table 4) shows that Lake Ulaan is highly sensitive to ongoing climate changes of precipitation, air temperature, and wind velocity. Lake Ulaan has experienced dramatic fluctuations of its extent over several thousand years. A giant paleolake of ~43 m depth might have existed at OSL-dated  $162 \pm 13$  ka, i.e., the paleolake formed after the Marine Isotope Stage (MIS) 6 (Lehmkuhl et al. 2018a; Table 4). The early time of a large lake covering an area of 19,000 km<sup>2</sup> being associated with wetter climates corresponded to a water level at 1285 m a.s.l. (Sternberg and Paillou 2015; Table 4). Then the lake was defined as an intermediate-sized lake covering a surface of ~6,900 km<sup>2</sup> at a water elevation of 1150 m a.s.l. (Sternberg and Paillou 2015; Table 4); however, the precise ages of such extended lakes are still unclear.

In the Holocene, the lake reduced to 1,700 km<sup>2</sup> in the area, corresponding to a water level at 1070 m a.s.l. (Sternberg and Paillou 2015; Table 4) occurring as the stage of the lake before the present-day dry basin (Fig.

9). In the middle Holocene (Fig. 9a), Lake Ulaan occupied an area of approximately 500 km<sup>2</sup> in size (Lehmkuhl et al. 2018a; Table 4). In the late Holocene (Fig. 9b), Lake Ulaan may have been exposed aerially for the first time. It coincides with the desiccated Lake Bayan Tukhum at 3.5 cal. ka BP (Felauer et al. 2012), ~105 km south from Lake Ulaan. If the remobilized and redeposited sediments are taken into account, the lake has been re-exposed to wind deflations at 0.6–1.3 cal. ka BP for the sites LU18-1, 2, 4, except for deep sediments at 2.4 cal. ka BP for the site LU18-3 (Table 2, Fig. 9c).

In the Anthropocene, Lake Ulaan may still have been a permanent lake (Table 4, Fig. 9c). The most recent high stand before the 1960s was when the lake level was maintained 2–3 m above the present dry lake bottom (Lehmkuhl et al. 2018a). The lake condition in addition to the former lakes determined by Murzaev and Besimalov before the 1950s (Table 4) is in accordance with the climate condition of the wettest epoch from the 1940s to the 1950s, reconstructed by Fang et al. (2010). Recently, Lake Ulaan has abruptly dried out and shrunk with sharply dropped areas (e.g., Davaa, 2015; Orkhonselenge et al. 2018a, b), and the former lake floor is partly covered by sedge plants (Fig. 2c). Once the largest lake in the Gobi, Lake Ulaan was identified in 1991 but did not appear in the Landsat images since 2000 (Kang et al. 2015). According to Davaa (2015), Lake Ulaan disappeared in 2010 and recovered an area of 20.9 km<sup>2</sup> in 2013 (Table 4). The frequent shrinkage of the lake since the 1950s has contributed to the aerial exposition of the lake floor to wind deflation and rapid redeposition (Figs. 9c, 10).

Although Lake Ulaan has experienced fluctuations of shrinking and/or filling depending on the annual precipitation and temperature (Orkhonselenge et al. 2018a) since the 1950s, the lake has finally shifted to become a playa (Fig. 9c). This was due to the strong westerly wind effects exceeding 20–25 m/s (Amarjargal 2016) and extreme over usage of groundwater by mining operation in the basin in addition to the rapidly rising air temperature (Orkhonselenge et al. 2018a). The playa condition (Fig. 9c) is reflected in intensified aeolian sedimentations (Lehmkuhl et al. 2018a), chemical weathering (Fig. 7b), and the climate change from semiarid to arid conditions (Fig. 11).

Although the eastern part of the lake is occasionally filled by the pulsating sedimentations by Ongi River during the heavy rainfalls, the lake basin has been thoroughly exposed to the westerly wind deflations (Figs. 9, 10). When the eastern part of the lake fills with water by Ongi River, it feeds the western part temporarily through the only channels C2 and C3 in the spit (Figs. 3, 10). Ongi River may fill only the eastern part, but due to the spit's presence, the lake water needs to reach the spit height before the two systems start connecting to each other fully. It implies that the filling of the western part should be delayed even though the groundwater feeds it (Fig. 10). The present playa condition of Lake Ulaan (Fig. 9c) is consistent with numerous other observations showing that most lakes in the eastern Gobi have been exposed aerially and dried out entirely due to the recent rapid rise in air temperature and evaporation during the last two decades (Orkhonselenge et al. 2019).

### 5.3 Holocene climate changes

In Mongolia, there is a common trend with the warm and humid early Holocene, the humid early to middle Holocene, the arid middle Holocene, and the humid late Holocene reconstructed paleoclimate records (An et al. 2008). However, the Holocene climate change has differed in each region of Mongolia. For instance, the

middle Holocene climate was recorded as humid in southern Mongolia and as arid in western Mongolia with well-developed ~9 m deep Lake Bayan Tukhum in southern Mongolia and a younger shallow Lake Ereen in western Mongolia (Grunert et al. 2009; Table 5). Moreover, the late Holocene climate in Mongolia was found as humid in northern Mongolia, and as an arid in southern Mongolia started since ~3.2 cal. ka BP and strengthened since 1.5 cal. ka BP (Orkhonselenge et al. 2018b; Table 5). The late Holocene climate in southern Mongolia at 1.5 cal. ka BP is more comparable with the results from northern China, while the paleoclimate pattern in northern Mongolia is much closer to the records from southern Siberia (Orkhonselenge et al. 2018b). In terms of the Holocene climate change in Mongolia, the climate in northern Mongolia has been remarkably in agreement with the paleoclimate changes in the East Asian winter monsoon (EAWM) and the mid-latitude westerlies dominated regions, whereas the climate in southern Mongolia has been coincident with the East Asian summer monsoon (EASM) and the westerlies dominated areas. For instance, the Holocene climate in the Govi region in southern Mongolia, including the Lake Ulaan area, coincides with the paleoclimate records from the EASM areas (Chen et al. 2008), showing a humid early Holocene and a drier late Holocene.

During the early Holocene, the paleoclimate in the Govi region is described relatively well (Table 5, Fig. 12). In the early Holocene, a humid and warm climate was recorded in lakes of southern Mongolia (e.g., Felauer et al. 2012; Lehmkuhl et al. 2018a). For example, Lake Ulaan contained an extensive network of paleohydrological complex (Holguin and Sternberg 2016) with a large area of 1,700 km<sup>2</sup> in the early Holocene (Sternberg and Paillou 2015). This coincided with the most humid time in the Lake Ulaan area because the EASM occurred in the north of Lake Ulaan at that time (Lee et al. 2013; Fig. 12). Since the beginning of the Holocene, there had been a reduction in sediment yield due to vegetation cover in the lakes within the Valley of Lakes (Lehmkuhl and Lang 2001), where fluvial sands were in dominant production (Lehmkuhl et al. 2018a). Around ~8.5 ka BP lakes in the Valley of Lakes were extended (Lehmkuhl and Lang 2001) and held high water levels in the early Holocene (Komatsu et al. 2001).

In the middle Holocene, the paleoclimate in the Valley of Lakes in southern Mongolia is shown as a continuation of the humid early Holocene (Table 5, Fig. 12), i.e., it was humid between 11.0 and 4.0 cal. ka BP (Felauer et al. 2012). The humid climate at 6.0–2.7 cal. ka BP caused the high sedimentation rate of 4.6 cm/ka in the lake's margin for the western part of Lake Ulaan (Orkhonselenge et al. 2018b; Figs. 9a, 12). It matched with the wet climate predominated at 8.6–4.7 cal. ka BP in the Lake Ulaan area (Lee et al. 2013). Lake levels in the Valley of Lakes were high (Grunert et al. 2009; Lehmkuhl et al. 2018a) because the northern limit of the EASM around the north of Lake Ulaan was close to the southern Khangai Mountain Range, and it ended at 4.0 ka BP (Lee et al. 2013; Fig. 12). The presence of the EASM around the Lake Ulaan area is consistent with the stronger EASM system during the middle Holocene contributed to the high precipitation, high water tables, and the halophytic desert vegetation growing around saline ponds in the Ikh Nart area (Rosen et al. 2019), locating at the higher latitude than that of Lake Ulaan. The humid middle Holocene revealed at Lake Ulaan coincided with the evidence of relatively higher lake levels during the middle Holocene recorded at Lakes Dood, Khuvsgul and Gun (Dorofeyuk and Tarasov 1998) in northern Mongolia, and Lakes Uvs and Bayan (Grunert et al. 2000) in the northern margin of the Depression of Great Lakes in western Mongolia (Orkhonselenge et al. 2018b). The high lake levels throughout most of arid Central Asia, recorded at

8.5 and 6.0 cal. ka BP (Li and Morril 2010) may have been related to the high precipitation associated with the westerlies increased from the early to middle Holocene (Chen et al. 2008).

The late Holocene climate in the Govi region is recorded from lakes as arid (Table 5, Figs. 9b, 11, 12). The dry climate is shown by numerous studies in southern Mongolia (e.g., Felauer et al. 2012; Szumińska 2016). The dry climate since 3.2–2.7 cal. ka BP in the Lake Ulaan basin may have induced the slow sedimentation rate of 1.6–1.8 cm/ka in the western part of Lake Ulaan (Orkhonselenge et al. 2018b) and strengthened the recent shrinkage of the shallow lake (Fig. 9b, c), a phenomenon seems to be continuing up to the modern time. The dry climate in the Lake Ulaan basin (Figs. 9b, c, 11, 12) coincides with the weakened EASM after 4.3 cal. ka BP contributed to the vegetation changing into an increase of steppe grasses in the Ikh Nart area (Rosen et al. 2019) in the northeastern Govi. Moreover, the late Holocene dry climate in the Govi region (Table 5, Figs. 11, 12) has contributed to have the lakes to be dried out and exposed to wind deflations (Grunert et al. 2009), and the arid and warm climate after 4.0 ka BP has influenced aeolian activity and dune remobilization (Felauer et al. 2012). The reactivation in the Khongor sand dunefield of the Govi region during the late Holocene representing the ongoing aridity (Hülle et al. 2010). In the arid late Holocene (Table 5, Fig. 12) Lake Ulaan may have been exposed to wind erosion since 3.2–2.7 cal. ka BP (Fig. 9b), and aeolian deflation has strengthened particularly since 0.6–1.3 cal. ka BP (Fig. 9c). The phenomena in the Lake Ulaan basin is in agreement with the desiccation of Lake Bayan Tukhum at 3.5 cal. ka BP (Felauer et al. 2012) and dried-out Lake Juyan in northern China during the last 2.0 ka BP (Chen et al. 2008). The strengthened arid climate in the Govi region since 1.5 cal. ka BP (Orkhonselenge et al. 2018b) prevailed during the periods before and after the time of high-standing lakes in the Valley of Lakes at 1.4–1.5 ka BP (Lehmkuhl and Lang 2001), and the more arid climate conditions during the late Holocene might have enhanced dust emission (Lehmkuhl 2015).

In the Anthropocene, the Govi region's climate is indicated as a dry (Table 5, Figs. 9c, 11). The trend in air temperature of the Govi region between 1961 and 2014 shows that the minimum air temperature in January was warmer than  $-21^{\circ}\text{C}$  in 1961–1987 and  $-19^{\circ}\text{C}$  in 1988–2014, whereas the maximum air temperature in July increased by  $2\text{--}3^{\circ}\text{C}$  (Dulamsuren 2016). A drought record from 1970 to 2006 across the Govi region using the Standard Precipitation Index (SPI) showed cyclical fluctuations with broadly wetter conditions in the 1970s and 1990s, a notably drier period in the 1980s and alternating wet-dry episodes in the 2000s, and an arid year in 2006 (Sternberg et al. 2011). The intense dryness or aridification causes the rapid shrinkage of lakes and a decrease in lake levels in the Govi regions (Figs. 2, 3, 9c, 11). The recent abrupt rising air temperature since 1995 and decreasing precipitation since 1987 in the Lake Ulaan area (Orkhonselenge et al. 2018a; Fig. 11) has caused the playa lake condition observed today (Fig. 9c). The trend is confirmed by a distinct tendency towards drier conditions since the 1980s reconstructed for the eastern central High Asia (Fang et al. 2010), and a statistically significant increase in the annual surface thawing index at a rate of  $29^{\circ}\text{C}\text{-days/yr}$  in Mongolia during the past 19 years, which is far greater than that in the high latitudinal regions of the Northern Hemisphere during recent decades (Wu et al. 2011).

By the end of this century, potential evaporation will rise by 200–300 mm/yr, with an increase in annual average surface temperature by  $5\text{--}6^{\circ}\text{C}$ , and the Govi region will extend 600 km toward the north (Dulamsuren 2016). This means that the present arid Govi region will shift into the dry desert, and the semiarid steppe regions will become arid Govi regions. This trend has been previously noted by Davi et al. (2015), showing

that the current drought conditions in Mongolia associated with annual average temperature increase by  $\sim 2^{\circ}\text{C}$  over the last 60 years have resulted in the expansion of desert areas from the warm and arid southern Mongolia towards central and northern regions of the country. The dry climate in the Govi region may rapidly contribute to the playa environments covering the semiarid steppe in a few years and result in a shortage of surface water resources, especially lakes and rivers. This trend has been confirmed by Lake Ulaan sediments showing the climate around the lake basin has been significantly shifted from the semiarid into the arid (Fig. 11).

## Conclusions

Late Holocene sedimentation records in Lake Ulaan at the eastern end of the Valley of Lakes at the northern border of the Govi region, southern Mongolia, show a higher sedimentation rate of 11.8–22.7 cm/ka in the eastern part of the lake and a lower sedimentation rate of 3.3–5.8 cm/ka in the western part of the lake. The lake has historically experienced a long-term evolution of a large lake since the initial formation after MIS 6 (Lehmkuhl et al. 2018a), and around that time, the lake reached the maximum size. In the context of lake retreats, the lake started to drop in the area before the early Holocene, strengthened the decreasing trend since the middle Holocene, and faced exposure to wind deflation in the late Holocene. The first aerial exposure occurred at 2.7–3.2 cal. ka BP and frequently exposed at 0.6–1.3 cal. ka BP. At the present time, the substantial westerly wind-induced aeolian deflation occurs throughout the lake bank even though the eastern part of the lake receives the pulsating fluvial sedimentations during heavy rainfall, and both parts receive aeolian air fall sedimentations. Today, Lake Ulaan has been remarkably reduced in extension and has rapidly shifted into a playa lake in the last five to six decades, and it has become an open-source area of dust generation blown out by the westerly winds.

## Declarations

The authors declare that they have no relevant financial or non-financial interests to disclose. The authors have no conflicts of interest to declare that are relevant to the content of this article.

## Acknowledgments

We would like to thank MSc D. Gerelsaikhan and BSc G. Tserendorj from the Laboratory of Geochemistry and Geomorphology (LGG), National University of Mongolia, for assisting our fieldwork. This work was supported by the National University of Mongolia (P2017-2388; P2017-2520). We especially thank Dr. G. Komatsu for valuable comments.

## Authors' contribution

All authors contributed to the study conception and design. Material preparation, data collection, mapping and analyses were performed by Alexander Orkhonselenge, Munkhjargal Uuganzaya and Tuyagerel Davaagatan. The original draft of the manuscript was written by Alexander Orkhonselenge, and all authors commented on the previous versions of the manuscript. All authors read, edited and approved the final manuscript.

## References

1. Abayomi E, Olatunji AS, Onashola B (2016) Inorganic geochemical evaluation and aspects of rock eval pyrolysis of Eocene to recent sediments of Soso and Kay-1 wells, western Niger delta, Nigeria. *J Env Ear Sci* 6(10):67–90.
2. Academy of Sciences of Mongolia, Academy of Sciences of USSR (1990) National Atlas of the Peoples' Republic of Mongolia. Ulaanbaatar, Moscow. [In Russian with English abstract]
3. Amarjargal D (2016) A relationship between weather condition and dust mobility in the Govi and steppe regions of Mongolia. Dissertation, National University of Mongolia. [In Mongolian]
4. An CB, Chen FH, Barton L (2008) Holocene environmental changes in Mongolia: A review. *Glo Plan Chan* 63:283–289. <https://doi.org/10.1016/j.gloplacha.2008.03.007>
5. Badarch G, Cunningham WD, Windley BF (2002) A new terrane subdivision for Mongolia: implications for the Phanerozoic crustal growth of Central Asia. *J Asi Ear Sci* 21:87–110. [https://doi.org/10.1016/S1367-9120\(02\)00017-2](https://doi.org/10.1016/S1367-9120(02)00017-2)
6. Baker VR (2007) Geology in Britannica. <https://www.britannica.com/science/playa>
7. Batima P, Natsagdorj L, Gomboluudev P, Erdenetsetseg B (2005) Observed climate change in Mongolia. AIACC Working Paper 12. [http://www.start.org/Projects/AIACC\\_Project/working\\_papers/Working%20Papers/AIACC\\_WP\\_No013.pdf](http://www.start.org/Projects/AIACC_Project/working_papers/Working%20Papers/AIACC_WP_No013.pdf)
8. Batnasan N (1998) Hydrological system, water regime, and evolution of large lakes in the Govi region. Dissertation, Institute of Geoecology, Mongolian Academy of Sciences. [In Mongolian]
9. Berkey PC, Morris KF (1927) Geology of Mongolia. The American Museum of Natural History, New York
10. Bridge J, Demicco R (2008) Earth Surface Processes, Landforms and Sediment Deposits. Cambridge University Press, UK
11. Bronk Ramsey C (2009) Bayesian analysis of radiocarbon dates. *Radiocarb* 51(1):337–360.
12. Chen F, Yu Z, Yang M, Ito E, Wang S, Madsen DB, Huang X, Zhao Y, Sato T, Birks HJB, Boomer I, Chen J, An C, Wunnemann B (2008) Holocene moisture evolution in arid central Asia and its out-of-phase relationship with Asian monsoon history. *Quat Sci Rev* 27:351–364. <https://doi.org/10.1016/j.quascirev.2007.10.017>
13. Dashzeveg D, Dingus L, Loope DB, Swisher CC, Dulam T, Sweeney MR (2005) New stratigraphic subdivision, epositional environment, and age estimate for the upper cretaceous Djadokhta formation, southern Ulan Nur basin, Mongolia. *Am Mus Novi* 3498:1–31. <http://hdl.handle.net/2246/5667>
14. Davaa, G., 2010. Climate Change Impacts on Water Resources in Mongolia. In: Institute for Global Environmental Strategies (Ed.), Integration of Climate Change Adaptation into Sustainable Development in Mongolia. Ulaanbaatar, pp. 30–36
15. Davaa G (2015) Resource and Regime of Surface Water of Mongolia. Admon, Ulaanbaatar. [In Mongolian]
16. Davi NK, D'Arrigo R, Jacoby GC, Cook ER, Anchukaitis K, Nachin B, Rao MP, Leland C (2015) A long-term context (931–2005 C.E.) for rapid warming over Central Asia. *Quat Sci Rev* 121:89–97. <https://doi.org/10.1016/j.quascirev.2015.05.020>

17. Dearing J (1994) Reconstructing the history of soil erosion. In: Roberts N (ed) The changing global environment. Blackwell, Oxford, pp 242–261
18. Dorofeyuk NI, Tarasov PE (1998) Vegetation and lake levels of northern Mongolia since 12,500 yr B.P. based on the pollen and diatom records. *Strat Geol Cor* 6(1):70–83.
19. Dulamsuren D (2016) Extreme air temperature changes and future of natural zone in Mongolia. Dissertation, National University of Mongolia. [In Mongolian]
20. Einsele G (1992) *Sedimentary basins: Evolution, Facies, and Sedimentary Budget*. Springer-Verlag, Berlin
21. Fang K, Davi N, Gou X, Chen F, Cook E, Li J, D'Arrigo R (2010) Spatial drought reconstructions for central High Asia based on tree rings. *Clim Dyn* 35:941–951. doi 10.1007/s00382-009-0739-9
22. Felauer T, Schultz F, Murad W, Mischke S, Lehmkuhl F (2012) Late Quaternary climate and landscape evolution in arid Central Asia: A multiproxy study of lake archive Bayan Tohomin Nuur, Gobi desert, southern Mongolia. *J Asi Ear Sci* 48:125–135. <https://doi.org/10.1016/j.jseaes.2011.12.002>
23. Fowell SJ, Hansen BC, Peck JA, Khosbayar P, Ganbold E (2003) Mid to late Holocene climate evolution of the Lake Telmen basin, north central Mongolia, based on palynological data. *Quat Res* 59(3):353–363. [https://doi.org/10.1016/S0033-5894\(02\)00020-0](https://doi.org/10.1016/S0033-5894(02)00020-0)
24. Grunert J, Lehmkuhl F, Walther M (2000) Paleoclimatic evolution of the Uvs Nuur basin and adjacent areas (Western Mongolia). *Quat Int* 65–66:171–192. [https://doi.org/10.1016/S1040-6182\(99\)00043-9](https://doi.org/10.1016/S1040-6182(99)00043-9)
25. Grunert J, Stolz C, Hempelmann N, Hilgers A, Hülle D, Lehmkuhl F, Felauer T, Dasch D (2009) The evolution of small lake basins in the Gobi desert in Mongolia. *Quat Sci* 29(4):678–689. <http://www.cnki.com.cn/Article/CJFDTotal-DSJJ200904004.htm>
26. Guy A, Schulmann K, Clauer N, Hasalová P, Seltmann R, Armstrong R, Lexa O, Benedicto A (2014) Late Paleozoic–Mesozoic tectonic evolution of the Trans-Altai and South Gobi Zones in southern Mongolia based on structural and geochronological data. *Gond Res* 25:309–337. <https://doi.org/10.1016/j.gr.2013.03.014>
27. Harnois L (1988) The CIW index: A new chemical index of weathering. *Sed Geol* 55(3–4):319–322. doi: [10.1016/0037-0738\(88\)90137-6](https://doi.org/10.1016/0037-0738(88)90137-6)
28. Hempelmann N (2010) Aeolian geomorphodynamics in endorheic basins of the Mongolian Gobi Desert. Dissertation, Mainz University
29. Herron MM (1988) Geochemical classification of terrigenous sands and shales from core or log data. *J Sed Pet* 58:820–829. <https://doi.org/10.1306/212F8E77-2B24-11D7-8648000102C1865D>
30. Holguin LR, Sternberg T (2016) A GIS based approach to Holocene hydrology and social connectivity in the Gobi Desert, Mongolia. *Arch Res Asi* 39:1–9. <https://doi.org/10.1016/j.ara.2016.12.001>
31. Hülle D, Hilgers A, Radtke U, Stolz C, Hempelmann N, Grunert J, Felauer T, Lehmkuhl F (2010) OSL dating of sediments from the Gobi Desert, Southern Mongolia. *Quat Geoch* 5:107–113. <https://doi.org/10.1016/j.quageo.2009.06.002>
32. Kang S, Lee G, Togtokh C, Jang K (2015) Characterizing regional precipitation-driven lake area change in Mongolia. *J Arid Land* 7(2):146–158. <https://doi.org/10.1007/s40333-014-0081-x>
33. Komatsu G, Brantingham PJ, Olsen JW, Baker VR (2001) Paleoshoreline geomorphology of Boon Tsagaan Nuur, Tsagaan Nuur and Orog Nuur: the Valley of Lakes, Mongolia. *Geom* 39:83–98.



[https://doi.org/10.1016/S0169-555X\(00\)00095-7](https://doi.org/10.1016/S0169-555X(00)00095-7)

34. Komatsu G, Ori GG, Marinangeli L, Moersch JE (2007) Playa environments on Earth: Possible analogues for Mars, In: Chapman MG (ed) *The Geology of Mars: Evidence from Earth-Based Analogs*, Cambridge University Press, pp 322–348
35. Lee MK, Lee YI, Lim HS, Lee JI, Choi JH, Yoon HI (2011) Comparison of radiocarbon and OSL dating methods for a Late Quaternary sediment core from Lake Ulaan, Mongolia. *J Paleolim* 45:127–135. doi:10.1007/s10933-010-9484-7
36. Lee MK, Lee YI, Lim HS, Lee JI, Yoon HI (2013) Late Pleistocene–Holocene records from Lake Ulaan, southern Mongolia: implications for east Asian palaeomonsoonal climate changes. *J Quat Sci* 28(4):370–378. <https://doi.org/10.1002/jqs.2626>
37. Lehmkuhl F (2015) Aeolian dust in mountain areas of Tibet and Mongolia. *ProSci* 1:44–50. doi:10.14644/dust.2014.008
38. Lehmkuhl F, Grunert J, Hülle D, Batkhishig O, Stauch G (2018a) Paleolakes in the Gobi region of southern Mongolia. *Quat Sci Rev* 179:1–23. <https://doi.org/10.1016/j.quascirev.2017.10.035>
39. Lehmkuhl F, Lang A (2001) Geomorphological investigations and luminescence dating in the southern part of the Khangay and the Valley of the Gobi Lakes (Central Mongolia). *J Quat Sci* 16(1):69–87. [https://doi.org/10.1002/1099-1417\(200101\)16:1<69::AID-JQS583>3.0.CO;2-O](https://doi.org/10.1002/1099-1417(200101)16:1<69::AID-JQS583>3.0.CO;2-O)
40. Lehmkuhl F, Nottebaum V, Hülle D (2018b) Aspects of late Quaternary geomorphological development in the Khangai Mountains and the Gobi Altai Mountains (Mongolia). *Geom* 312:24–39. <https://doi.org/10.1016/j.geomorph.2018.03.029>
41. Li Y, Morrill C (2010) Multiple factors causing Holocene lake-level change in monsoonal and arid central Asia as identified by model experiments. *Clim Dyn* 35:1119–1132. doi:10.1007/s00382-010-0861-8
42. Makhbadar Ts (2012) Mesozoic era. In: Byamba J (ed) *Geology and Mineral Resources of Mongolia: Stratigraphy*. Ulaanbaatar, pp. 417–510. [In Mongolian]
43. McGeehin J, Burr GS, Jull AJT, Reines D, Gosse J, Davis PT, Muhs D, Southon JR (2001) Stepped-combustion <sup>14</sup>C dating of sediment: a comparison with established techniques. *Radiocarb* 43(2A):255–261. <https://doi.org/10.1017/S003382220003808X>
44. McLennan SM, Hemming S, McDaniel DK, Nanson GN (1993) Geochemical approaches to sedimentation, provenance and tectonics. *Geol Soc Am: Spec Pap* 284:295–303.
45. Narantsetseg Ts, Badamgarav J, Ariunbileg S, Badamgarav D, Oyunchimeg Ts, Idermunkh T, Uugantsetseg B, Tuvshinjargal B, Dolgorsuren Kh (2011) *Geology of the Meso-Cenozoic depressions*. Institute of Geology and Mineral Resources, Ulaanbaatar. [In Mongolian]
46. Nesbitt HW, Young GM (1982) Early Proterozoic climates and plate motions inferred from major element chemistry of lutites. *Nature* 299:715–717. <https://link.springer.com/content/pdf/10.1038/299715a0.pdf>
47. Nesbitt HW, Young GM (1984) Prediction of some weathering trends of plutonic and volcanic rocks based on thermodynamic and kinetic considerations. *Geochi Cosmochi Acta* 48:1523–1534. [https://doi.org/10.1016/0016-7037\(84\)90408-3](https://doi.org/10.1016/0016-7037(84)90408-3)
48. Orkhonselenge A, Bukhchuluun D, Aca C, Odsuren D (2019) A brief preliminary report on fieldwork in Shiriin Chuluu area in the eastern Gobi in southeastern Mongolia. National University of Mongolia,

Ulaanbaatar.

49. Orkhonselenge A, Komatsu G, Uuganzaya M (2018a) Climate-driven changes in lake areas for the last half century in the Valley of Lakes, Govi region, southern Mongolia. *Nat Sci* 10(7):263–277. doi: [10.4236/ns.2018.107027](https://doi.org/10.4236/ns.2018.107027)
50. Orkhonselenge A, Komatsu G, Uuganzaya M (2018b) Middle to late Holocene sedimentation dynamics and paleoclimatic conditions in the Lake Ulaan basin, southern Mongolia. *Géomorph: rel, proc, env* 24(4):351–363. <https://journals.openedition.org/geomorphologie/12219>
51. Orkhonselenge A, Krivonogov SK, Mino K, Kashiwaya K, Safonova IY, Yamamoto M, Kashima K, Nakamura T, Kim JY (2013) Holocene sedimentary records from Lake Borsog, eastern shore of Lake Khuvsgul, Mongolia, and their paleoenvironmental implications. *Quat Int* 290–291:95–109. <https://doi.org/10.1016/j.quaint.2012.03.041>
52. Owen LA, Windley BF, Cunningham WD, Badamgarav J, Dorjnamjaa D (1997) Quaternary alluvial fans in the Gobi of southern Mongolia: evidence for neotectonics and climate change. *J Quat Sci* 12(3):239–252. [https://doi.org/10.1002/\(SICI\)1099-1417\(199705/06\)12:3<239::AID-JQS293>3.0.CO;2-P](https://doi.org/10.1002/(SICI)1099-1417(199705/06)12:3<239::AID-JQS293>3.0.CO;2-P)
53. Peck JA, Khosbayar P, Fowell SJ, Pearce RB, Ariunbileg S, Hansen BCS, Soninkhishig N (2002) Mid to Late Holocene climate change in north central Mongolia as recorded in the sediments of Lake Telmen. *Palaeogeogr, Palaeoclim, Palaeoeco* 183:135–153. [https://doi.org/10.1016/S0031-0182\(01\)00465-5](https://doi.org/10.1016/S0031-0182(01)00465-5)
54. Prokopenko AA, Kuzmin MI, Williams DF, Gelety VF, Kalmychkov GV, Gvozdkov AN, Solotchin PA (2005) Basin-wide sedimentation changes and deglacial lake-level rise in Lake Hovsgol basin, NW Mongolia. *Quat Int* 136:59–69. <https://doi.org/10.1016/j.quaint.2004.11.008>
55. Reimer PJ, Bard E, Bayliss A, Beck JW, Blackwell PG, Ramsey CB, Buck CE, Cheng H, Edwards RL, Friedrich M, Grootes PM, Guilderson TP, Hafliðason H, Hajdas I, Hatte C, Heaton TJ, Hoffmann DL, Hogg AG, Hughen KA, Kaiser KF, Kromer B, Manning SW, Niu M, Reimer RW, Richards DA, Scott EM, Southon JR, Staff RA, Turney CSM, van der Plicht J (2013) IntCal13 and Marine13 radiocarbon age calibration curves, 0–50,000 years cal BP. *Radiocarb* 55(4):1869–1887.
56. Roberts N (1998) *The Holocene: An Environmental History*. Blackwell, UK
57. Rosen AM, Hart TC, Farquhar J, Schneider JS, Yadmaa T (2019) Holocene vegetation cycles, land-use, and human adaptations to desertification in the Gobi Desert of Mongolia. *Veg Hist Archaeobot* 28:295–309. <https://link.springer.com/article/10.1007/s00334-018-0710-y>
58. Roser BP, Korsch RJ (1986) Determination of tectonic setting of sandstone-mudstone suites using SiO<sub>2</sub> content and K<sub>2</sub>O/Na<sub>2</sub>O ratio. *J Geol* 94:635–650. <https://www.journals.uchicago.edu/doi/pdf/10.1086/629071>
59. Roser BP, Korsch RJ (1988) Provenance signatures of sandstone-mudstone suites determined using discriminant function analysis of major-element data. *Chem Geol* 67(1–2):119–139. [https://doi.org/10.1016/0009-2541\(88\)90010-1](https://doi.org/10.1016/0009-2541(88)90010-1)
60. Sternberg T, Paillou P (2015) Mapping potential shallow groundwater in the Gobi Desert using remote sensing: Lake Ulaan Nuur. *J Arid Env* 118:21–27. <https://doi.org/10.1016/j.jaridenv.2015.02.020>
61. Sternberg T, Thomas D, Middleton N (2011) Drought dynamics on the Mongolian steppe, 1970–2006. *Int J Clim* 31:1823–1830. <https://doi.org/10.1002/joc.2195>

62. Stolz C, Hülle D, Hilgers A, Grunert J, Lehmkuhl F, Dasch D (2012) Reconstructing fluvial, lacustrine and aeolian process dynamics in Western Mongolia. *Zeit Geomorph* 56(3):267–300.
63. Stuiver M, Polach HA (1977) Discussion: Reporting of  $^{14}\text{C}$  data, *Radiocarb* 19(3):355–363.
64. Suttner LJ, Dutta PK (1986) Alluvial sandstone composition and paleoclimate, I. Framework mineralogy. *J Sed Pet* 56:329–345. <https://doi.org/10.1306/212F8909-2B24-11D7-8648000102C1865D>
65. Szumińska D (2016) Changes in surface area of the Böön tsagaan and Orog lakes (Mongolia, Valley of the lakes, 1974–2013) compared to climate and permafrost changes. *Sed Geol* 340:62–73. <https://doi.org/10.1016/j.sedgeo.2016.03.002>
66. Tsegmid Sh (1969) *Physical Geography of Mongolia*. State Press, Ulaanbaatar. [In Mongolian]
67. Tsend N (1965) Water chemical composition of lakes in the Govi region. Institute of Livestock, Ulaanbaatar. [In Mongolian]
68. Tserensodnom J (1971) *Lakes of Mongolia*. State Press, Ulaanbaatar. [In Mongolian]
69. Tserensodnom J (2000) *A catalog of lakes in Mongolia*. Shuvuun Saaral, Ulaanbaatar. [In Mongolian]
70. Watanabe T, Nakamura T, Nara FW, Kakegawa T, Horiuchi K, Senda R, Oda T, Nishimura M, Matsumoto GI, (2009) High-time resolution AMS  $^{14}\text{C}$  data sets for Lake Baikal and Lake Hovsgol sediment cores: changes in radiocarbon age and sedimentation rates during the transition from the last glacial to the Holocene. *Quat Int* 205:12–20. <https://doi.org/10.1016/j.quaint.2009.02.002>
71. Wu T, Wang Q, Zhao L, Batkhishig O, Watanabe M (2011) Observed trends in surface freezing/thawing index over the period 1987–2005 in Mongolia. *Cold Reg Sci Tech* 69:105–111. <https://doi.org/10.1016/j.coldregions.2011.07.003>

## Figures

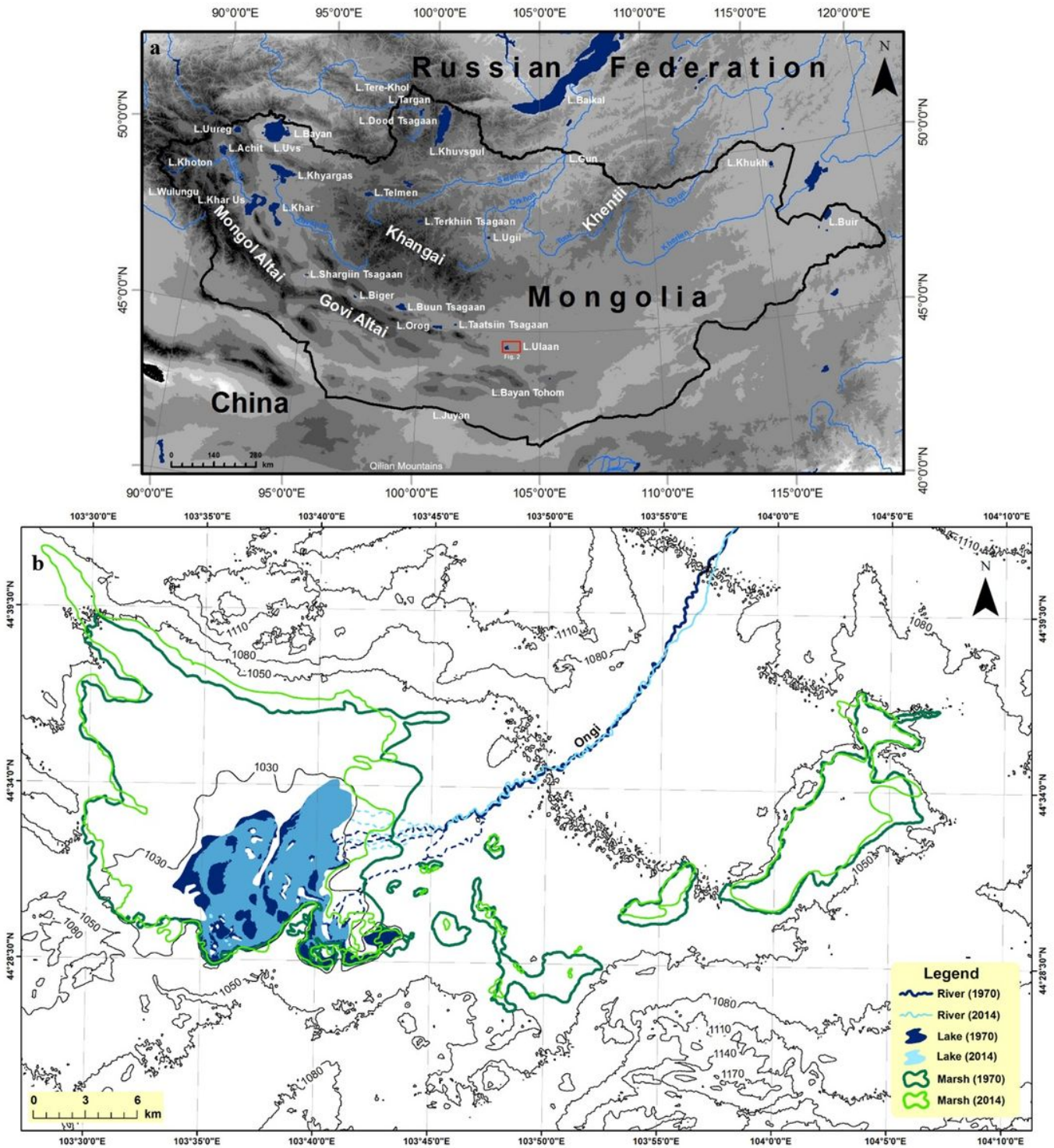


**Figure 1**

(a) Geographical location of Lake Ulaan in the northern margin of the Govi region in southern Mongolia. (b) Spatial changes in lake and marsh areas in the Lake Ulaan basin in 1970 and 2014. Modified from Orkhonselenge et al. (2018b) Note: The designations employed and the presentation of the material on this map do not imply the expression of any opinion whatsoever on the part of Research Square concerning the legal status of any country, territory, city or area or of its authorities, or concerning the delimitation of its frontiers or boundaries. This map has been provided by the authors.

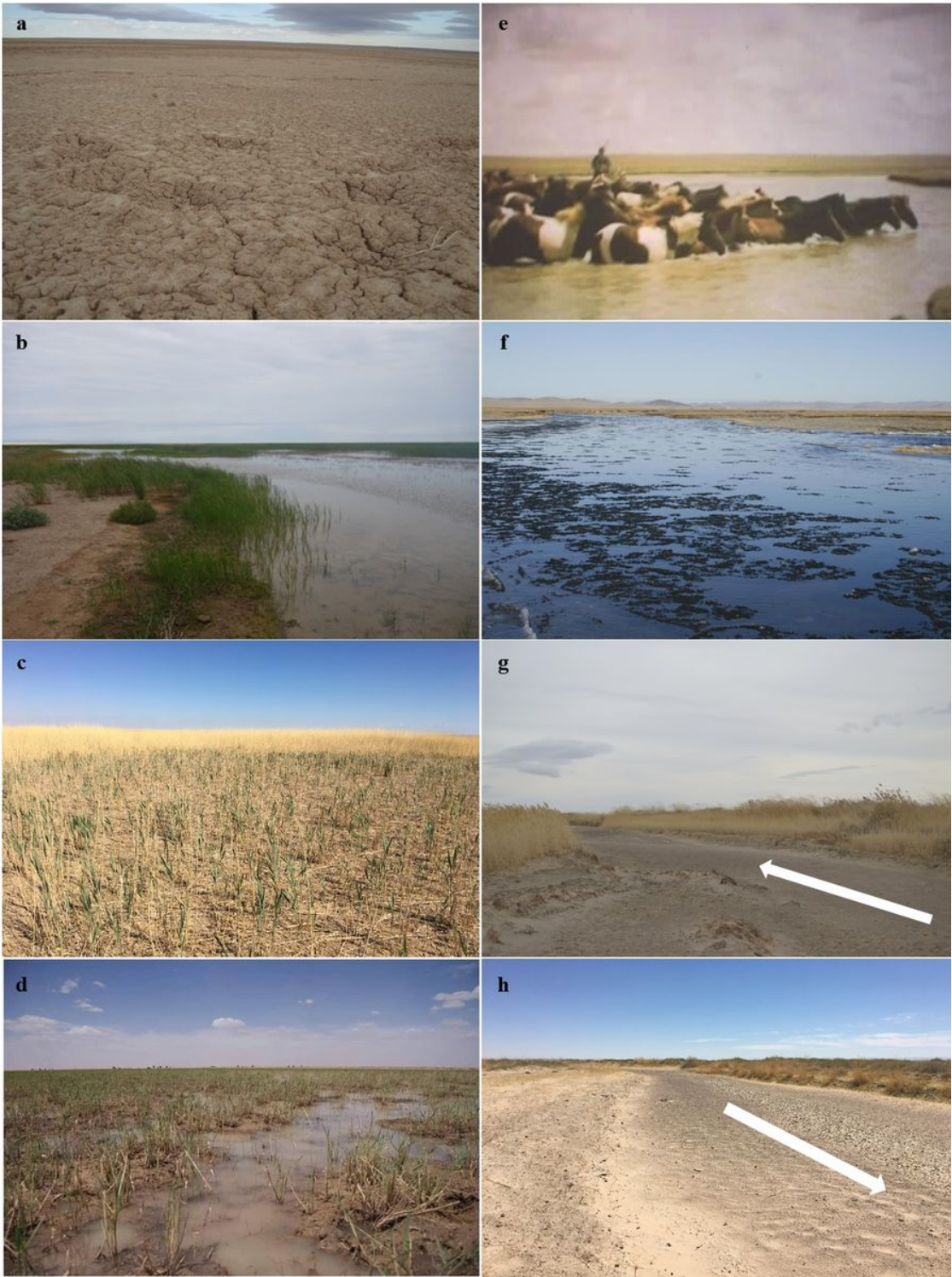


**Figure 2**

Temporal views of Lake Ulaan (LU) and Ongi River (OR) in the last decade except for a record in 1980. (a) The exposed floor of LU viewing toward the southwest on 25 October 2015. (b) LU in August 2016. (c) Exposed vegetated floor of LU viewing toward the south on 18 June 2018. (d) LU on 23 June 2019. (e) OR in 1980. (f) OR on 14 June 2012. (g) A dried-out channel of OR viewing toward the east on 25 October 2015. (h) A dried-out channel of OR viewing toward the northwest on 18 June 2018. The arrows in g and h show the flow

direction of Ongi River. Photos a, c, g, h by A. Orkhonselenge. Photo b by Holgium and Sternberg (2016). Photo d by E. Suvdaa. Photos e, f by Ongi River Movement Non-Governmental Organization

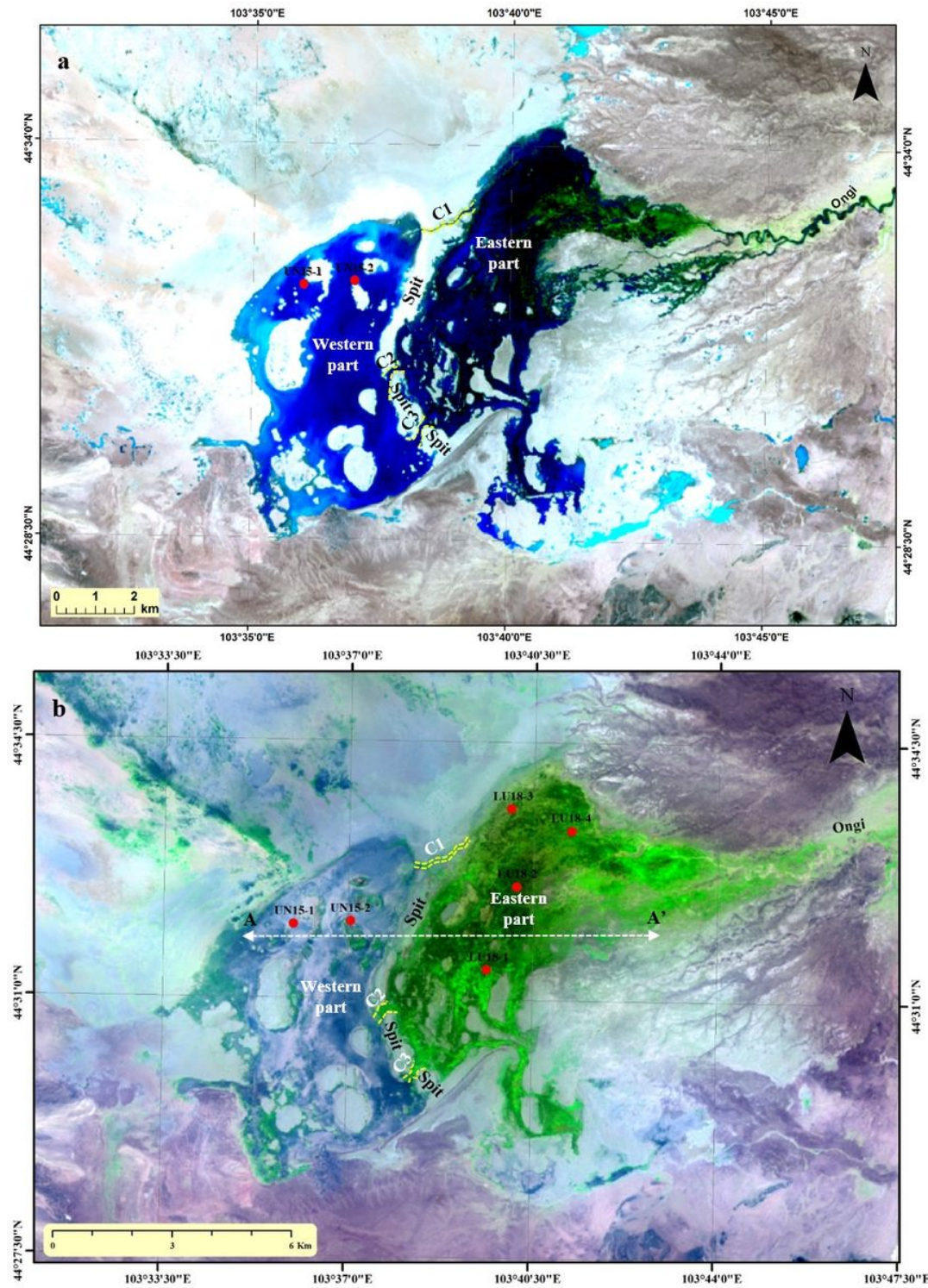


**Figure 3**

Sampling sites on Landsat images of Lake Ulaan in (a) 2014 and (b) 2019 Note: The designations employed and the presentation of the material on this map do not imply the expression of any opinion whatsoever on the part of Research Square concerning the legal status of any country, territory, city or area or of its

authorities, or concerning the delimitation of its frontiers or boundaries. This map has been provided by the authors.

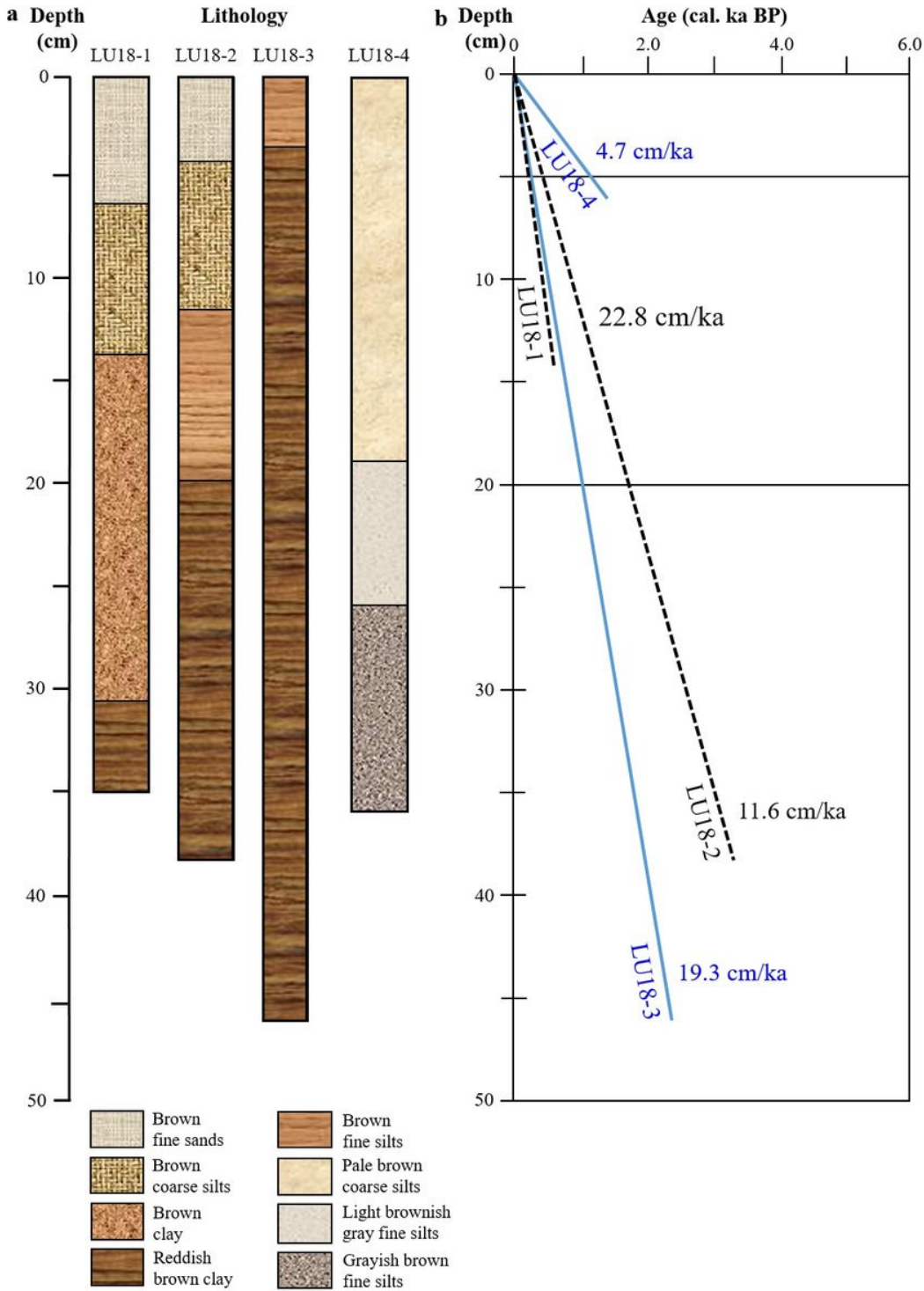


**Figure 4**

(a) The lithology of sediment cores collected in 2018 and (b) the sedimentation rates in Lake Ulaan

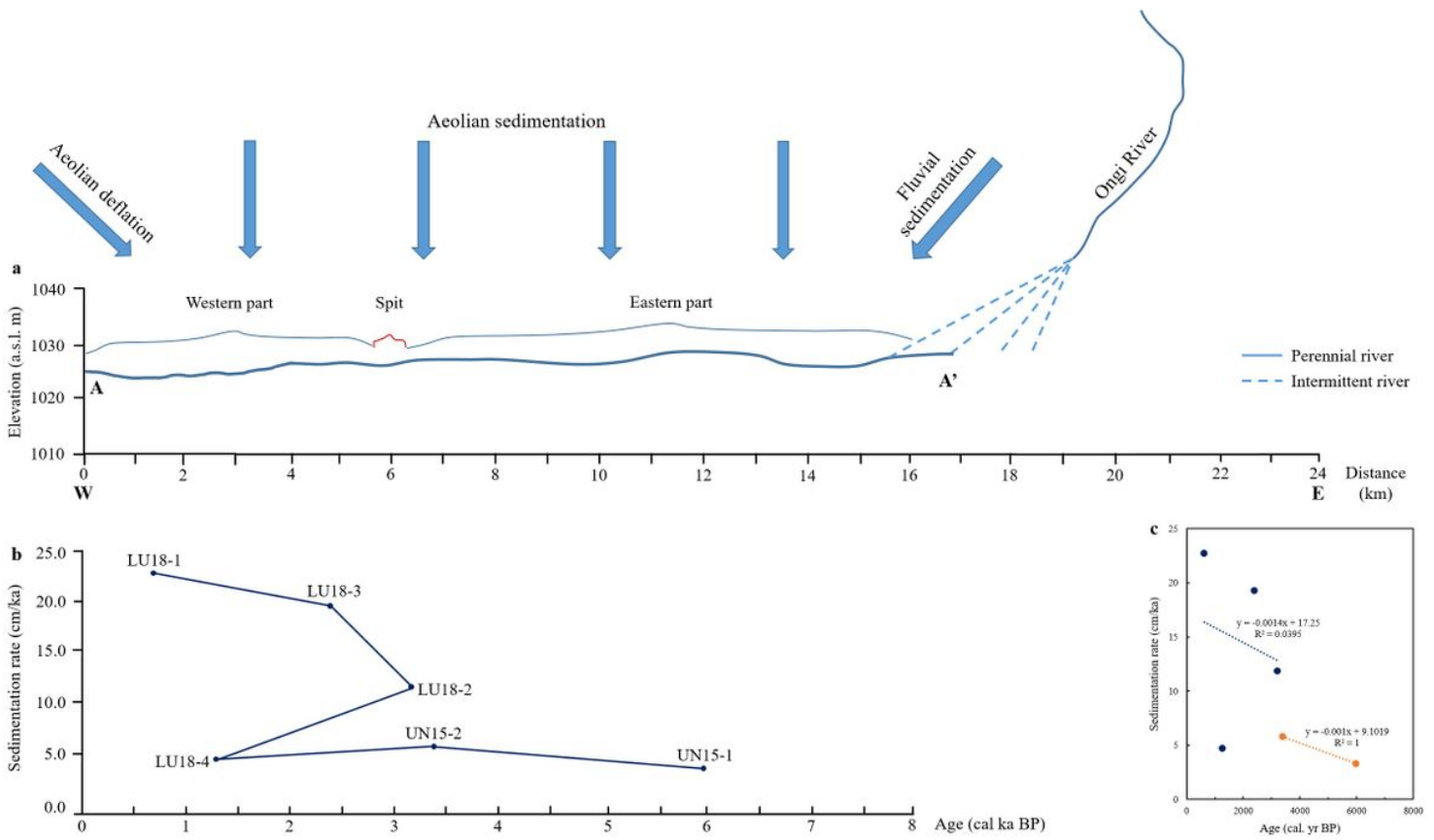


**Figure 5**

(a) Discriminant function (F1 and F2) diagram for the four types of provenance signatures of Lake Ulaan sediments using major element compositions, and (b) tectonic setting diagram for the Lake Ulaan sediments: oceanic island arc (ARC), active continental margin (ACM) and passive margin (PM) settings



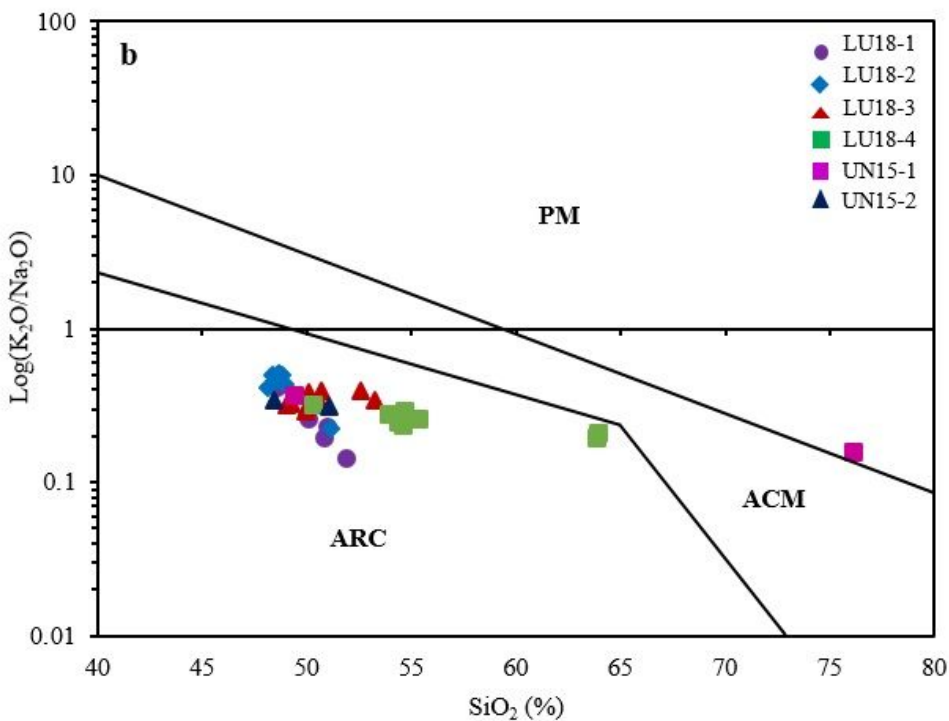
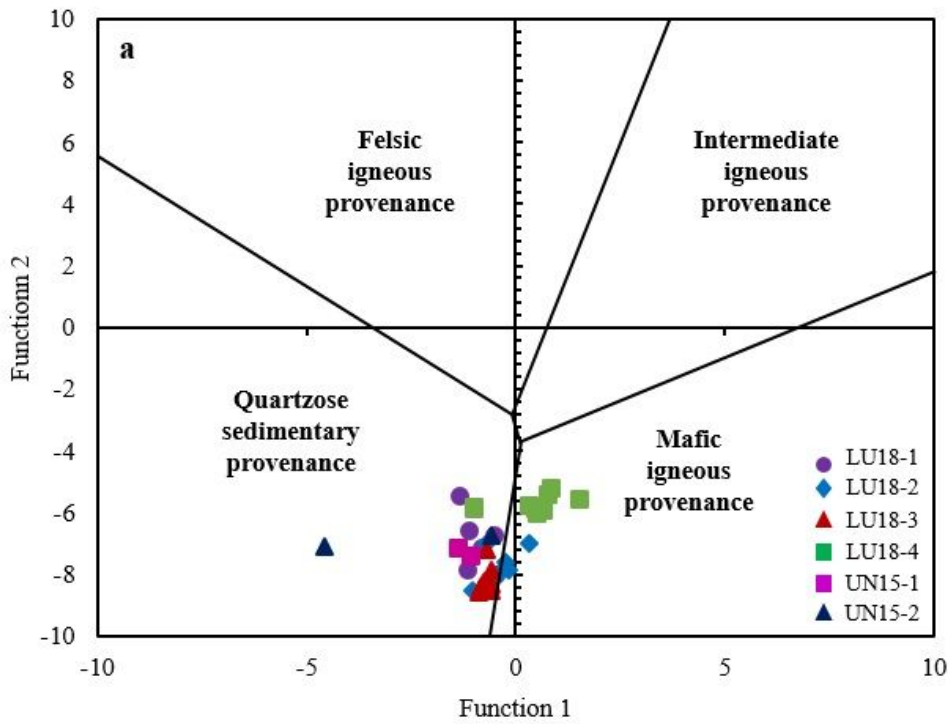


**Figure 6**

(a) Geochemical classification of the Lake Ulaan sediments based on the  $\log[\text{SiO}_2/\text{Al}_2\text{O}_3]$  vs.  $\log[\text{Fe}_2\text{O}_3/\text{K}_2\text{O}]$  diagram. (b) A-CN-K ( $\text{Al}_2\text{O}_3\text{-CaO}+\text{Na}_2\text{O-K}_2\text{O}$ ) ternary diagram showing the weathering trend of the Lake Ulaan sediments with Ka (Kaolinite), Ch (Chlorite), Gb (Gibbsite), Il (Illite), Ms (Muscovite), Kf (K-feldspar), Sm (Smectite), Pl (Plagioclase), To (Tonalite), Gd (Granodiorite), Gr (Granite), and Ga (Gabbro)

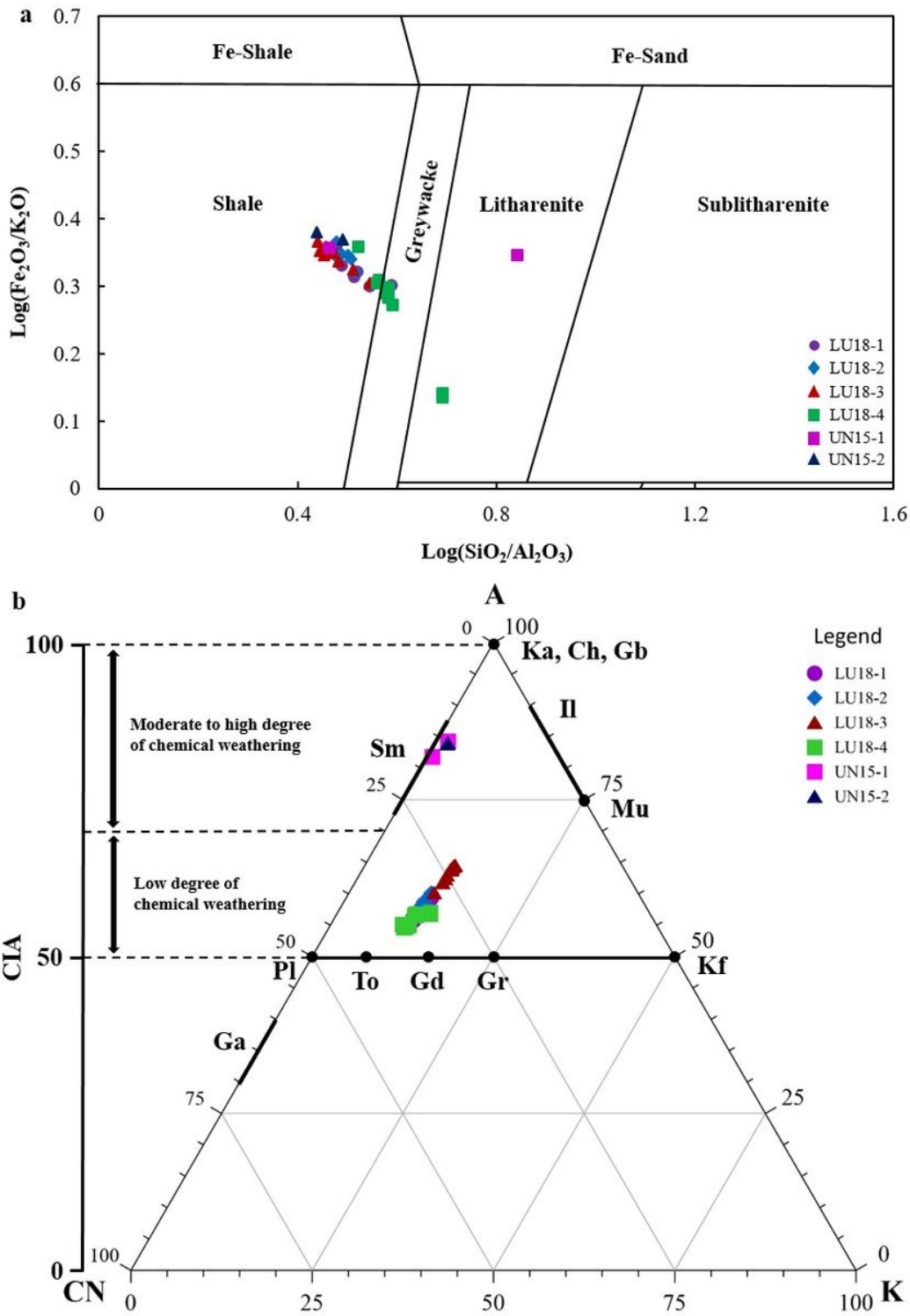


**Figure 7**

Sedimentation dynamics in Lake Ulaan with (a) a cross-section of the lake, (b) Holocene sedimentation rate, and (c) Linear regressions of the sedimentation rate in the late Holocene for cores UN15 in the west and LU18 in the east of the lake

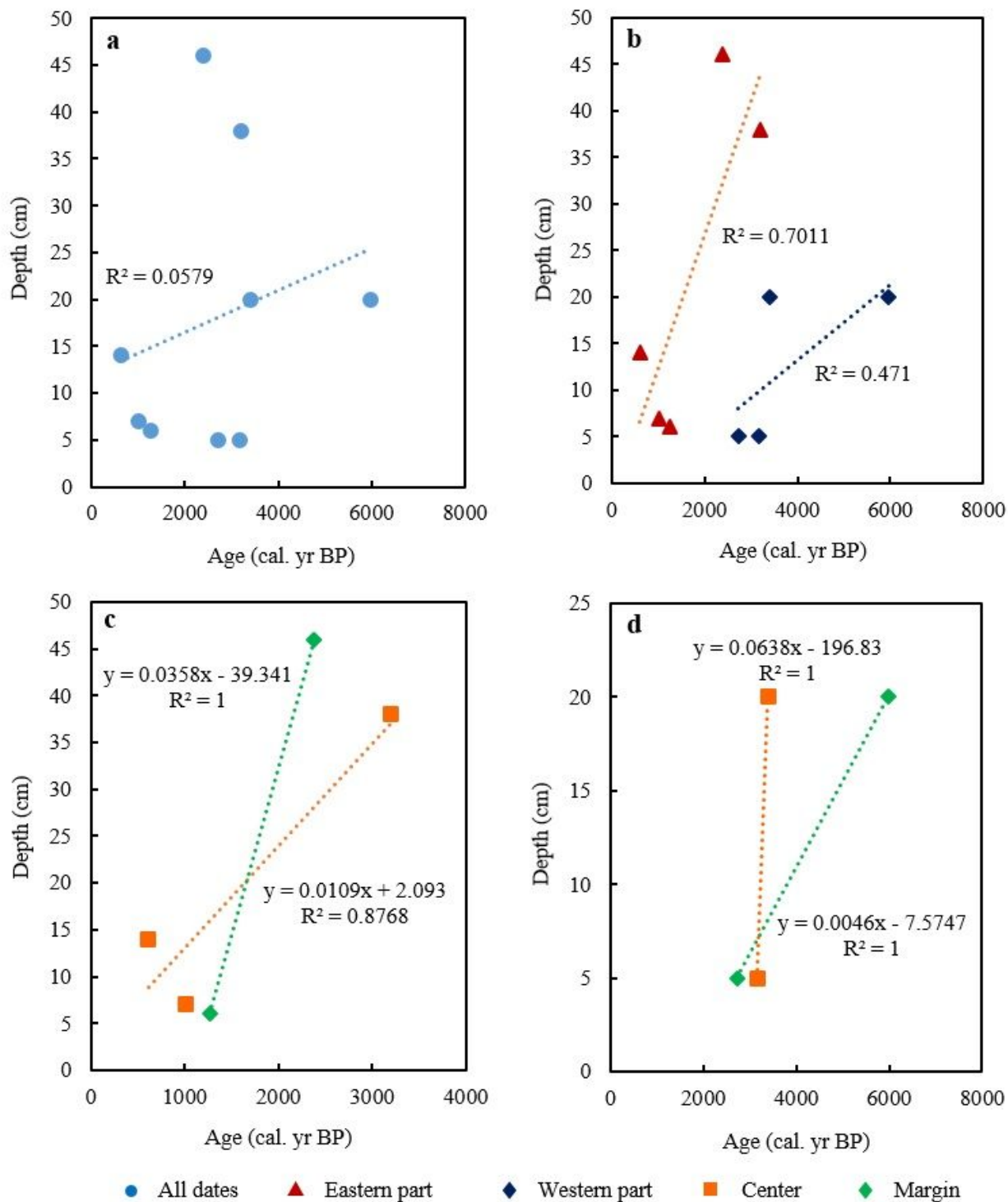


**Figure 8**

The age to depth model in (a) Lake Ulaan, specified with (b) the eastern and western parts of the lake, (c) the center and margin in the eastern part of the lake, and (d) the center and margin in the western part of the lake in Orkhonselenge et al. (2018b)

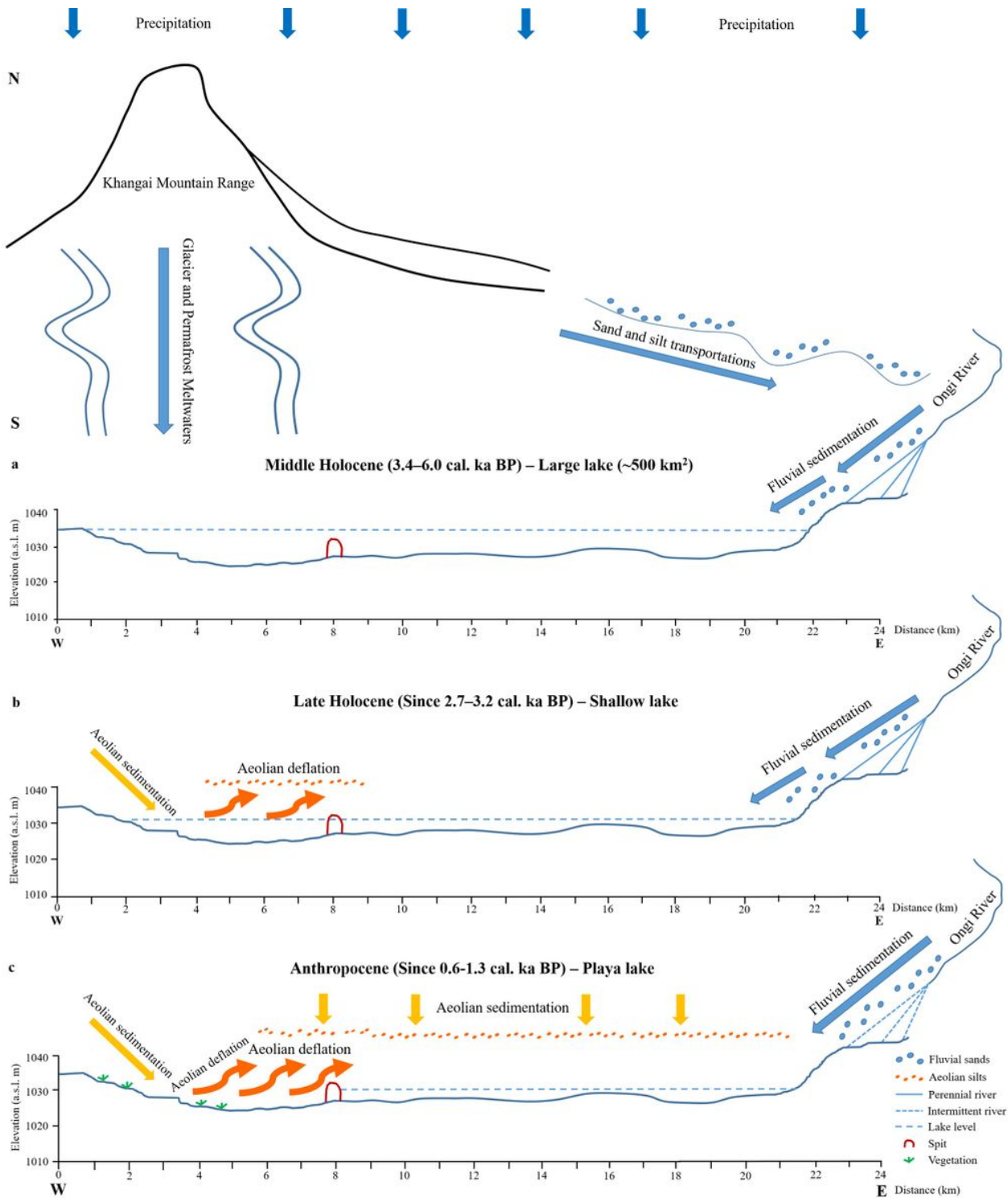


**Figure 9**

Schematic diagrams illustrating the historical evolution of Lake Ulaan in the (a) middle Holocene, (b) late Holocene, and (c) Anthropocene

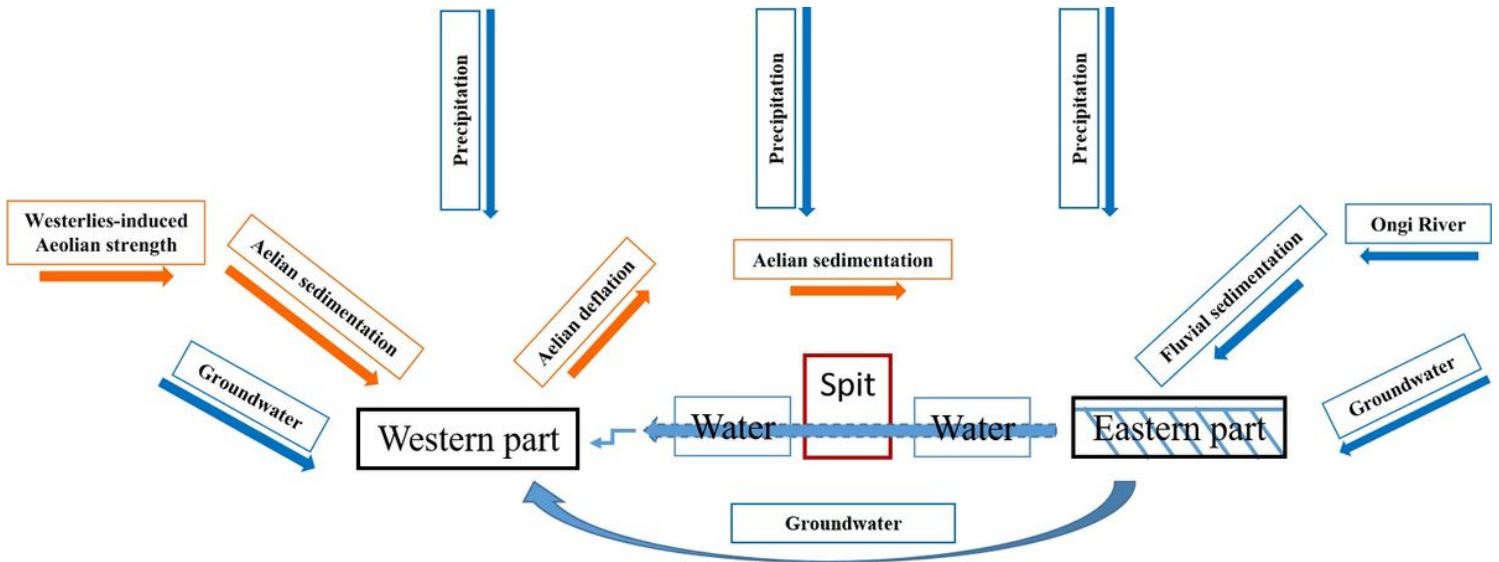


Figure 10

A hypothesized model on how the western part of Lake Ulaan is fed by spillover through the channels (C1 to C3) over the spit after the eastern part is filled by water through Ongi River

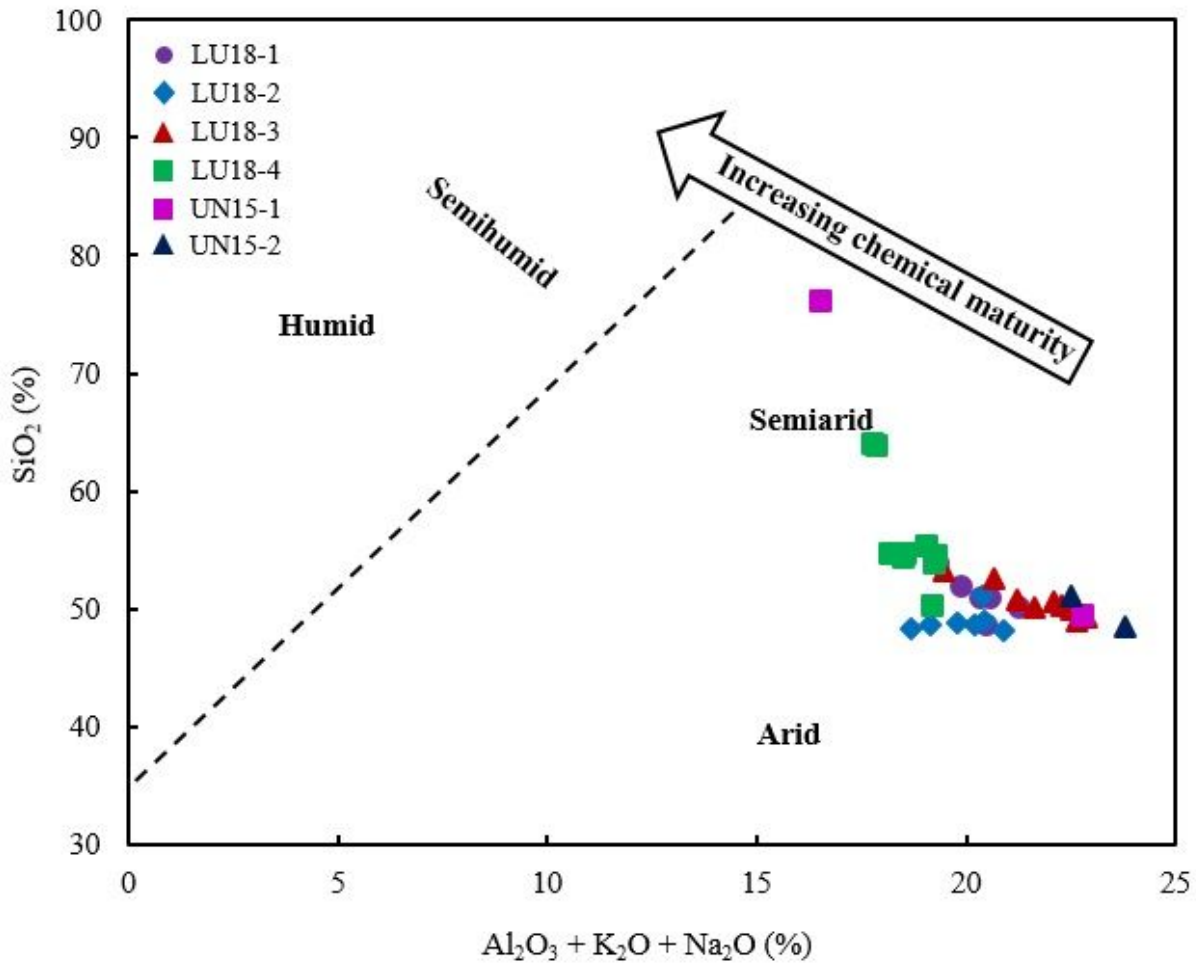


Figure 11

Chemical maturity of Lake Ulaan sediments by a plot of SiO<sub>2</sub> vs. Al<sub>2</sub>O<sub>3</sub>+K<sub>2</sub>O+Na<sub>2</sub>O

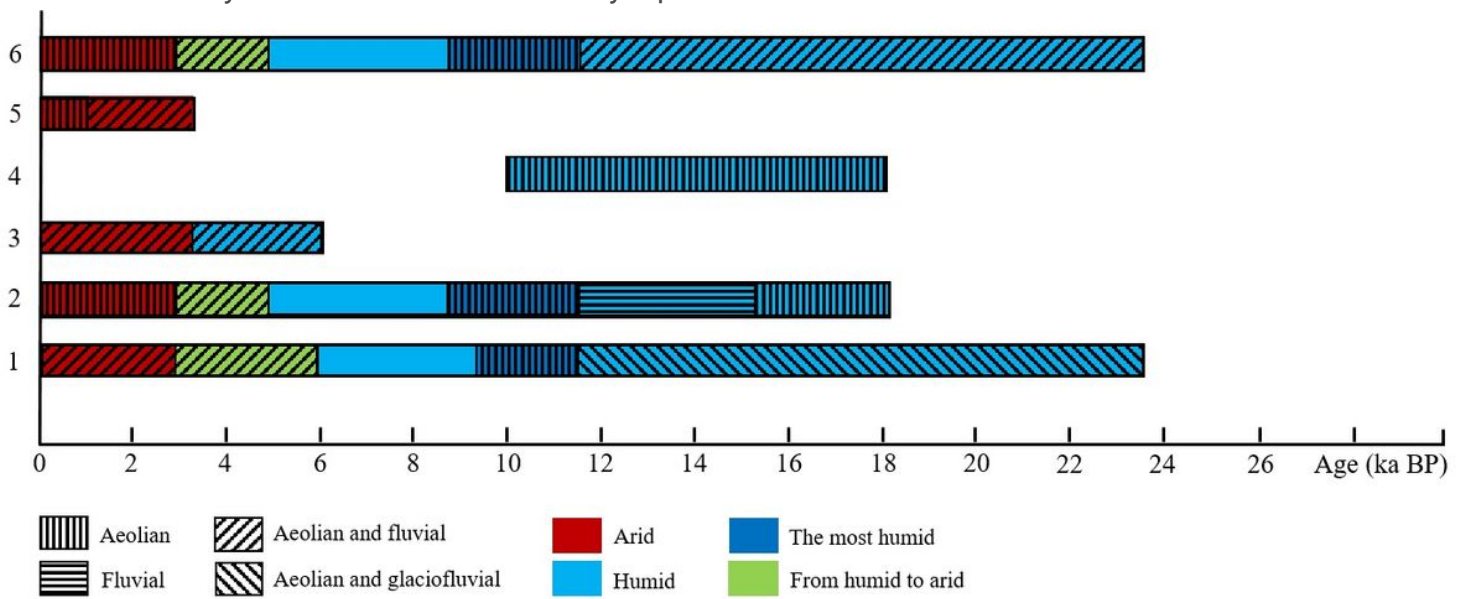


Figure 12

The dominant sedimentations and paleoclimate changes in the Lake Ulaan basin since the late Pleistocene: 1 – Lee et al. (2011), 2 – Lee et al. (2013), 3 – Orkhonselenge et al. (2018b), 4 – Lehmkuhl et al. (2018a), 5 – This study, and 6 – Synthesized trend